

RESEARCH

Developing a prognostic model for biochemical recurrence in prostate cancer using a novel circRNA-miRNA-mRNA regulatory network

Barry Digby^{1*}, Stephen P. Finn² and Pilib Ó Broin¹

Abstract

Background: Biochemical recurrence (BCR) occurs in one-third of prostate cancer patients treated with local therapy and inevitably develops in all patients treated with enzalutamide. In this study, we combined both PCa and enzalutamide-resistance signatures to derive a model for effective prediction of BCR in prostate cancer.

Methods: Differentially expressed circRNAs, miRNAs and mRNAs were incorporated from multiple studies to derive a competing endogenous RNA (ceRNA) regulatory network. A prognostic model was constructed from the network using Cox regression and stepwise regression. The model was further tested on six external validation datasets to evaluate the efficacy of the prognostic model in predicting BCR. Pathway analysis and immune infiltration analysis was computed on a per-sample basis to identify differences in high-risk and low-risk patients.

Results: The linear predictors from the 4-gene prognostic model effectively stratified patients into high-risk and low-risk strata with significantly different BCR outcomes. High-risk patients exhibited unfavourable prognosis and elevated immune infiltration compared to low-risk groups. Moreover, the prognostic model exhibited high prediction accuracy in classifying patients with BCR events in both the derivation and validation datasets.

Conclusion: We present a first-of-kind circRNA-miRNA-mRNA regulatory network derived from prostate cancer and enzalutamide-resistant cells. The prognostic ceRNA network offers insights into the potential regulatory mechanism of non-coding RNAs in BCR.

Keywords: Prostate cancer; Enzalutamide; Biochemical recurrence; Prognostic signature; Competing endogenous RNA network

Background

Prostate cancer (PCa) is the second most frequent cancer and the fifth leading cause of cancer-associated deaths in men [1]. Radical prostatectomy, external beam radiotherapy or brachytherapy are the mainstay of treatment for localized PCa. Approximately 35% of men experience biochemical recurrence (BCR) after treatment as defined by three consecutive rises in prostate-specific antigen (PSA) levels 1 week apart, progressing to castrate-resistant PCa (CRPC) [2]. Treatment courses for CRPC involve the abrogation of androgen receptor (AR) signalling, preventing its translocation to the nucleus and binding to DNA [3]. Enzalutamide is one such second-generation anti-

androgen drug that competitively binds the ligand binding domain of the AR impeding AR signalling. Despite overall survival benefits of 4.8 months in patients, between 20% - 40% are intrinsically resistant whilst all will eventually acquire resistance to the drug as measured by increasing PSA levels [2,4] indicative of BCR. There is therefore an increasing need to identify biomarkers associated with BCR in CRPC and enzalutamide-resistant patients.

Next generation sequencing (NGS) provides researchers with a powerful tool to detect biomarkers in clinical samples. The preparation times, sequencing time and costs associated with NGS technologies are constantly dropping, making NGS a cost-effective tool for biomarker discovery [17]. RNA biomarkers are of particular interest, providing a snapshot of the dynamic cellular states compared to DNA biomarkers and exhibit superior sensitivity and specificity com-

*Correspondence: b.digby1@universityofgalway.ie

¹School of Mathematical and Statistical Sciences, University of Galway, Galway, Ireland

Full list of author information is available at the end of the article

Table 1 Prostate cancer datasets used in the study.

Data type	Series	Platform	Sample size tumor	Sample size normal
circRNA	GSE113153 [5]	GPL21825	10	0
miRNA	GSE21036 [6]	GPL8227	100	28
miRNA	GSE23022 [7]	GPL8786	20	20
miRNA	GSE36803 [8]	GPL8786	21	21
miRNA	GSE45604 [9]	GPL14613	50	10
miRNA	GSE46738 [10]	GPL8786	53	4
miRNA	TCGA [11]	PRAD	498	52
mRNA	TCGA [11]	PRAD	498	52

Table 2 Enzalutamide datasets used in the study.

Data type	Series	Platform	Description of LNCaP samples
circRNA	GSE118959 [12, 13]	GPL21825	Clone 1, Clone 9, Control (n=3)
miRNA	<i>in-house</i>	Illumina TruSeq	Clone 1, Clone 9, Control (n=3)
mRNA	GSE143408 [14]	GPL25684	21, 14, 7, 0 days Enz trt (n=3)
mRNA	GSE78201 [15]	GPL10558	6 months Enz trt, control (n=4)
mRNA	GSE88752 [16]	GPL11154	Enz trt, Enz sensitive (n=4)
mRNA	<i>in-house</i>	Illumina NovaSeq	Clone 1, Clone 9, Control (n=3)

pared to protein biomarkers [18, 19]. Taken together, RNA biomarkers not only provide clinical utility but can also refine our knowledge of underlying disease aetiology.

The ENCODE project revealed 76% of the human genome is transcribed, but only 1.2% of this represents protein-coding genes [20, 21] resulting in an increased interest in non-coding RNAs (ncRNAs) and their role in gene regulation. ncRNAs can be categorised as small ncRNAs (<200nt length) comprising micro RNAs (miRNAs), piwi-interacting RNAs (piRNAs), small nucleolar RNAs (snoRNAs) and long non-coding RNAs (lncRNAs) (> 200nt length). More recently, circular RNAs (circRNAs), originally believed to be aberrant by-products of splicing [22, 23], have emerged as a class of ncRNAs. circRNAs harbour functionally active and evolutionarily conserved miRNA response elements (MRE) within their mature spliced sequence capable of sequestering miRNAs and have been proposed to act as competitive endogenous RNAs (ceRNAs) in circRNA-miRNA-mRNA regulatory networks [24–26]. Several studies detailing the role of ncRNAs in PCa have since emerged, identifying potential molecular biomarkers, new therapeutic strategies and advancing our understanding of disease progression [27–31].

The tumor microenvironment (TME) represents a complex ecosystem of neoplastic cells, extracellular matrix (ECM), and nonneoplastic cells, including resident mesenchymal support cells, endothelial cells, and infiltrated inflammatory immune cells. Whether by cause or consequence, aberrant innate and adaptive immune responses contribute to the tumorigenesis of early stage cancers by applying selective pressure to tumor cells, preferentially selecting aggressive clones, inducing immunosuppression and stimulating tumor

cell proliferation [32]. In clinically detectable cancers, T cell infiltration has been reported to improve patient outcomes [33]. Conversely, macrophage populations (M2-like polarisation) are associated with worse outcome [34]. It is therefore of interest to characterise the immune cell subpopulations to identify putative markers for disease progression. Whilst progress has been made on this front in studies of the PCa TME, results are largely conflicting owing to the heterogeneous nature of PCa [35].

In this study, we combine multiple circRNA, miRNA, mRNA PCa and enzalutamide-resistant expression datasets to derive a competing endogenous RNA (ceRNA) network. Using the mRNAs in the network, we derived a prognostic signature for the prediction of BCR in patients using The Cancer Genome Atlas Prostate Adenocarcinoma (TCGA-PRAD) dataset. The effectiveness of the prognostic signature was demonstrated using TCGA-PRAD and six external PCa datasets, where patients were stratified into high-risk and low-risk categories showing distinctly different BCR outcomes. By combining the prognostic index obtained from the 4-gene prognostic signature with clinical features, we derived a clinical nomogram for clinical use. Furthermore, we detail the TME in high-risk and low-risk stratum via immune infiltration analysis to add to the growing knowledge base of immune-cell based biomarkers in PCa.

Methods

Data collection

The Gene Expression Omnibus (GEO) [36] (<https://www.ncbi.nlm.nih.gov/geo/>) was used to access publicly available microarray and RNA-Sequencing datasets that contain circRNA, miRNA and mRNA

expression profiles of prostate cancer patients and LNCaP cell lines treated with enzalutamide. circRNA microarray datasets were screened using the search term ("GPL21825[Accession] AND ("prostatic neoplasms"[MeSH Terms] OR prostate cancer[All Fields]) AND ("g se"[Filter] AND "Non-coding RNA profiling by array"[Filter]))". miRNA datasets were screened using the search term ("prostate"[MeSH Terms] OR prostate[All Fields]) AND ("micrornas"[All Fields] OR "micrornas"[MeSH Terms] OR miRNA[All Fields]) AND LNCaP[All Fields]"). Finally, mRNA datasets were screened using the search term ("enzalutamide"[All Fields] OR ("enzalutamide"[All Fields] OR enzalutamide[All Fields]) AND "LNCaP"[All Fields] AND "gse"[Filter]).

In addition to the selected GEO datasets, TCGA-PRAD miRNA and mRNA expression datasets were downloaded from the GDC portal [11] (<https://portal.gdc.cancer.gov/>) on July 25th 2023. In-house sequencing of enzalutamide-resistant LNCaP cell lines was performed to generate miRNA and mRNA expression data to supplement the construction of the circRNA-miRNA-mRNA network. Descriptions of samples used in each dataset for differential expression analysis and network construction are provided (Table 1, Table 2).

With respect to modelling a prognostic signature, the TCGA-PRAD mRNA dataset was used as the derivation dataset. The Belfast (GSE116918 [37]), CPC (GSE107299 [38]), DKFZ (EGAS00001002923 [39]), Long et al. 2014 (GSE54460 [40]), Taylor et al. 2010 (GSE21034 [41]), Ross-Adams et al. 2014 (Stockholm, GSE70769 [42]) PCa datasets were used as validation datasets for the prognostic model.

Data processing and differential expression analysis of circRNAs, miRNAs and mRNAs

GSE113153, GSE118959, GSE45604, GSE46738, GSE-143408 and GSE78201 quantile normalized log2 transformed circRNA, miRNA and mRNA microarray datasets were downloaded using GEOquery [43] and analysed in R (version 4.2.0). GSE21036, GSE23022 and GSE36803 miRNA and mRNA raw CEL files were downloaded from ArrayExpress [44] (<http://www.ebi.ac.uk/arrayexpress>), requiring log2 RMA normalization using the oligo package [45] prior to differential expression analysis. GSE88752, TCGA-PRAD miRNA and TCGA-PRAD mRNA count data were normalized with respect to library size using edgeR [46] and transformed using limma-voom [47]. In-house LNCaP small RNA-Sequencing data was processed in the following manner: 1) download, process and generate indices using the miRBase hairpin FASTA file [48,49]; 2) removal of adapter sequences and read filtering [50]; 3) collapse filtered reads [51]; 4) align collapsed reads to the hairpin [48]; 5) quantify miRNAs using miRBase GFF file

[52]. The in-house LNCaP RNA-Sequencing samples were processed using the 'STAR-Salmon' transcript quantification subworkflow in nf-core/rnaseq [53].

Limma [54] was used to identify differentially expressed circRNAs/miRNAs/mRNAs between contrasts of interest; genes with an adjusted p-value ≤ 0.05 after Benjamini-Hochberg multiple testing correction were deemed statistically significant. Candidate circRNA/miRNA/mRNAs identified by differential expression analysis for network construction were screened by the following criteria: 1) circRNAs must be present in GSE118959 Clone 1 vs. control (high enzalutamide resistance) and one of GSE118959 Clone 9 vs. control (moderate enzalutamide resistance) or GSE113153 Gleason high ≥ 8 vs. Gleason low <8 ; 2) miRNAs must be present in LNCaP Clone 1 vs. control (high enzalutamide resistance) and at least one of GSE21036, GSE23022, GSE36803, GSE46738, GSE46738 or TCGA-PRAD (tumor vs. normal); 3) mRNAs must be present in LNCaP Clone 1 vs. control (high enzalutamide resistance), TCGA-PRAD (tumor vs. normal) and one of GSE88752, GSE143408, GSE78201 enzalutamide-resistant datasets. 4) common circRNAs/miRNAs/mRNAs identified must exhibit the same fold-change direction in the limma topTable results from which they originate. Customised scripts were used to convert both Arraystar human circRNA microarray V2 probes to circbase IDs and outdated miRNA probe IDs to the latest miRBase alias to ensure standardization of results and compatibility with downstream target prediction analysis.

circRNA, miRNA, mRNA target prediction

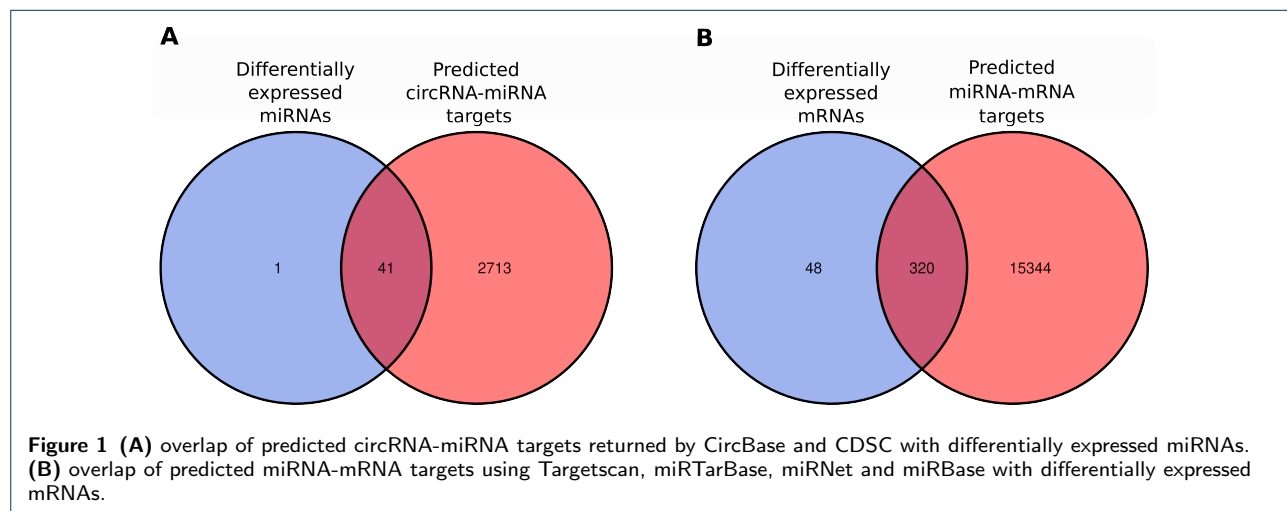
The predicted targets of screened differentially expressed (DE) circRNAs were obtained using the CircBase database [55] (<http://www.circbase.org/>) and the Cancer-Specific CircRNA Database [56] (<http://gb.whu.edu.cn/CSCD/>), generating database-guided circRNA-miRNA pairs. Candidate DE-miRNAs for the ceRNA network were subset via the intersection of the predicted circRNA-miRNA targets. Finally, the gene targets of DE-miRNAs were obtained using miRBase [57] (<https://www.mirbase.org/>), miRTarBase [58] (<https://mirtarbase.cuhk.edu.cn/>), miRNet [59] (<https://www.mirnet.ca/miRNet/home.xhtml>) (a user-submitted list of miRNAs) and TargetScan [60] (https://www.targetscan.org/vert_80/) and overlapped with DE-mRNAs for ceRNA network construction.

Construction of ceRNA network

Using R, the ceRNA network was subject to a final round of filtering to conform to the hypothesized sponging model between circRNA, miRNAs and mRNAs: 1) the higher the circRNA expression, the lower

Table 3 Differentially expressed RNAs returned by Limma.

Data type	Series	Contrast	Up-regulated	Down-regulated
circRNA	GSE113153	Gleason high vs. low	2761	2245
circRNA	GSE118959	Clone 1 vs. control	649	771
circRNA	GSE118959	Clone 9 vs. control	20	79
		Unique overlapping circRNAs:	174	105
miRNA	GSE21036	Tumor vs. normal	153	146
miRNA	GSE23022	Tumor vs. normal	17	8
miRNA	GSE36803	Tumor vs. normal	36	92
miRNA	GSE45604	Tumor vs. normal	22	67
miRNA	GSE46738	Tumor vs. normal	68	68
miRNA	LNCaP	Clone 1 vs. control	146	110
miRNA	LNCaP	Clone 9 vs. control	4	1
miRNA	TCGA-PRAD	Tumor vs. normal	130	128
		Unique overlapping miRNAs:	16	26
mRNA	GSE143408	7 days vs. 0 days	3829	3458
mRNA	GSE143408	14 days vs. 0 days	5693	4792
mRNA	GSE143408	21 days vs. 0 days	6128	4977
mRNA	GSE78201	6 months vs. control	518	571
mRNA	GSE88752	ADT + ENZ vs. control	3564	2942
mRNA	LNCaP	Clone 1 vs. control	4686	4379
mRNA	LNCaP	Clone 9 vs. control	1420	1303
mRNA	TCGA-PRAD	Tumor vs. normal	3860	4506
		Unique overlapping mRNAs:	196	172



the miRNA expression and higher the mRNA expression; 2) the lower the circRNA expression, the higher the miRNA expression and lower the mRNA expression. A nodelist and edgelist was exported and visualised using Cytoscape software [61] (version 3.10.0 <https://cytoscape.org/>).

Enrichment Analysis

Active-subnetwork-oriented pathway enrichment analysis was performed on DE-mRNAs in the ceRNA network using pathfindR [62]. KEGG, Reactome and GO gene sets were used to identify active subnetworks (in which interconnected genes predominantly comprise input DE-mRNAs) in the BioGrid protein-protein interaction network (PIN) over 100 iterations. Enriched

pathways with a p-value ≤ 0.05 and ≥ 50 occurrences over all iterations were considered significant. Hierarchical clustering was performed on all enriched terms using 1 - kappa statistic as the distance metric to generate a network cluster. The network was rearranged to include clusters with the largest membership in Inkscape vector graphics software.

Construction of a prognostic model

To assess the prognostic value of the DE-mRNAs returned by the ceRNA network, univariate Cox proportional hazards regression and Benjamini Hochberg multiple testing correction ($P \leq 0.05$) was conducted using the RegParallel R package [63] on scaled and centred log2 CPM TCGA-PRAD gene expression data

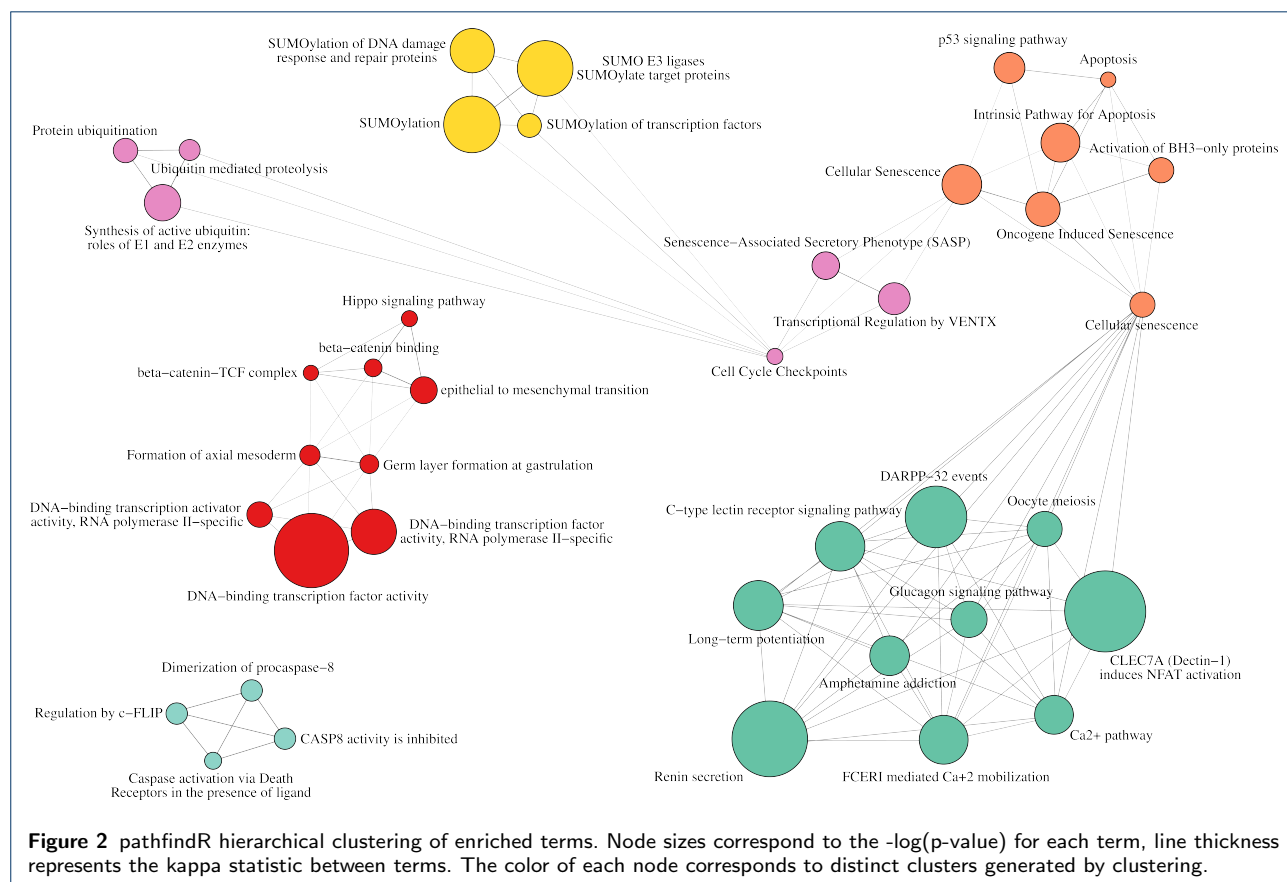


Figure 2 pathfindR hierarchical clustering of enriched terms. Node sizes correspond to the $-\log(p\text{-value})$ for each term, line thickness represents the kappa statistic between terms. The color of each node corresponds to distinct clusters generated by clustering.

to identify biochemical recurrence (BCR) associated genes. Genes that violated the proportional hazard assumptions as determined by scaled Schoenfeld residuals [64] were discarded. Next, we constructed a multivariate Cox proportional hazards model using backwards selection via the stepwise Akaike information criterion (stepAIC) MASS function [65] with a significance level of $P \leq 0.05$ to identify the most relevant predictors.

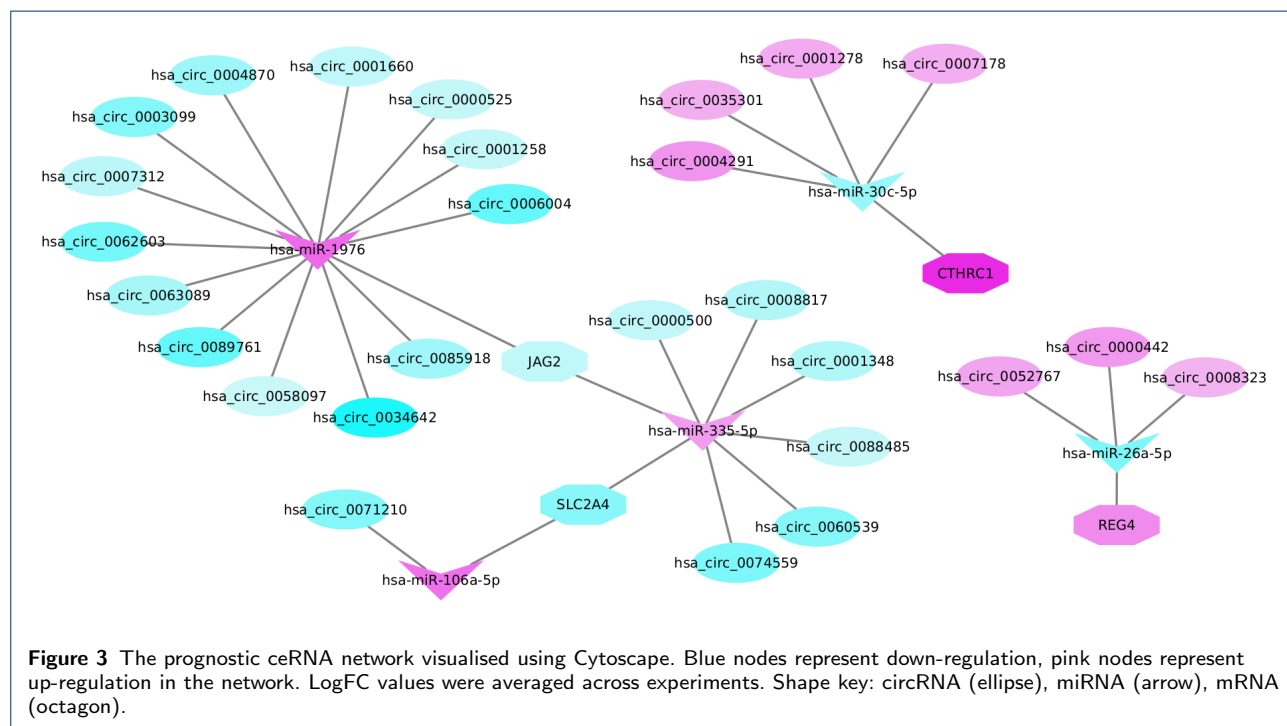
A prognostic index (PI) was constructed using the weighted sum of the variables in the model, where the weights are the regression coefficients. The median value of the PI was used to stratify patients into high risk and low-risk strata with the expectation that the high risk group would harbour more biochemical recurrence events and thus have a poorer prognosis than the low-risk group. Kaplan-Meier survival analysis and a log-rank test was employed to formally assess this assumption using the survfit function in the survminer R package [66]. Furthermore, the timeROC R package [67] was used to show receiver operating characteristic (ROC) curves, and area under ROC curve (AUC) to evaluate the prediction of the prognostic model for 1, 3, 5 and 8 years biochemical recurrence rates, respectively.

Construction of a clinical nomogram

A univariate and multivariate cox proportional hazards model was constructed to include PI and the clinical covariates age, PSA, Gleason score, pathologic T, pathologic N, clinical M and surgical resection status. To reduce the degrees of freedom in the model, the covariates age, Gleason score and PSA were stratified to produce the categorical variables: age ≥ 56 / <56 ; Gleason score ≤ 6 , Gleason score 7 and Gleason score 8, 9 and 10; PSA $<10\text{ng/ml}$, PSA 10-20ng/ml and PSA $>20\text{ng/ml}$. The optimal cutoff for age was calculated using the maxstat R package [68]. Furthermore, pathologic T was simplified to T2, T3 and T4 status. Next, the transcan function in the Hmisc R package [69] was used to impute missing values in each covariate before fitting a univariate and multivariate cox regression model. Significant covariates ($P \leq 0.05$) with a positive hazard ratio were included in the final nomogram model. The nomogram was constructed using the RMS R package [70] and visualized using the regplot R package [71]. The prediction accuracy of the overall nomogram and each of its individual predictors was calculated for years 1, 3, 5 and 8 in the TCGA-PRAD dataset via AUC. Furthermore, Harrell's c-index was

Table 4 4-gene prognostic model obtained from the ceRNA network.

Gene	Coef	CI	exp(Coef)	S.E.	Wald Z	P-value
REG4	-0.392	(-0.602, -0.181)	0.676	0.107	-3.65	0.00026
SLC2A4	-0.293	(-0.509, -0.076)	0.746	0.111	-2.64	0.0082
JAG2	0.394	(0.185, 0.603)	1.483	0.107	3.69	0.00022
CTHRC1	0.419	(0.196, 0.640)	1.520	0.113	3.71	0.00021



calculated and compared to the derivation model to assess the clinical models performance.

Model validation on external datasets

To validate the 4 gene prognostic model using external datasets, we calculated the discriminative power and overall model fit as suggested in a previous review [72] in conjunction with ROC analysis to assess model performance: 1) The calibration slope in the validation dataset was computed and compared to the slope of the derivation dataset. A calibration slope <1 suggests less discriminative power whilst a slope >1 indicates superior discriminative power in the validation dataset. 2) The overall fit of the prognostic model in the validation dataset was computed via a joint test of all predictors whilst constraining the prognostic index to 1. A small Chi-squared test value and non-significant p-value indicate a good fit of the prognostic index in the validation dataset. 3) Harrell's c-index was computed for both the derivation and validation datasets; agreement between the two datasets being indicative of similar predictive performance. 4) Kaplan-Meier survival curves between risk group strata, as de-

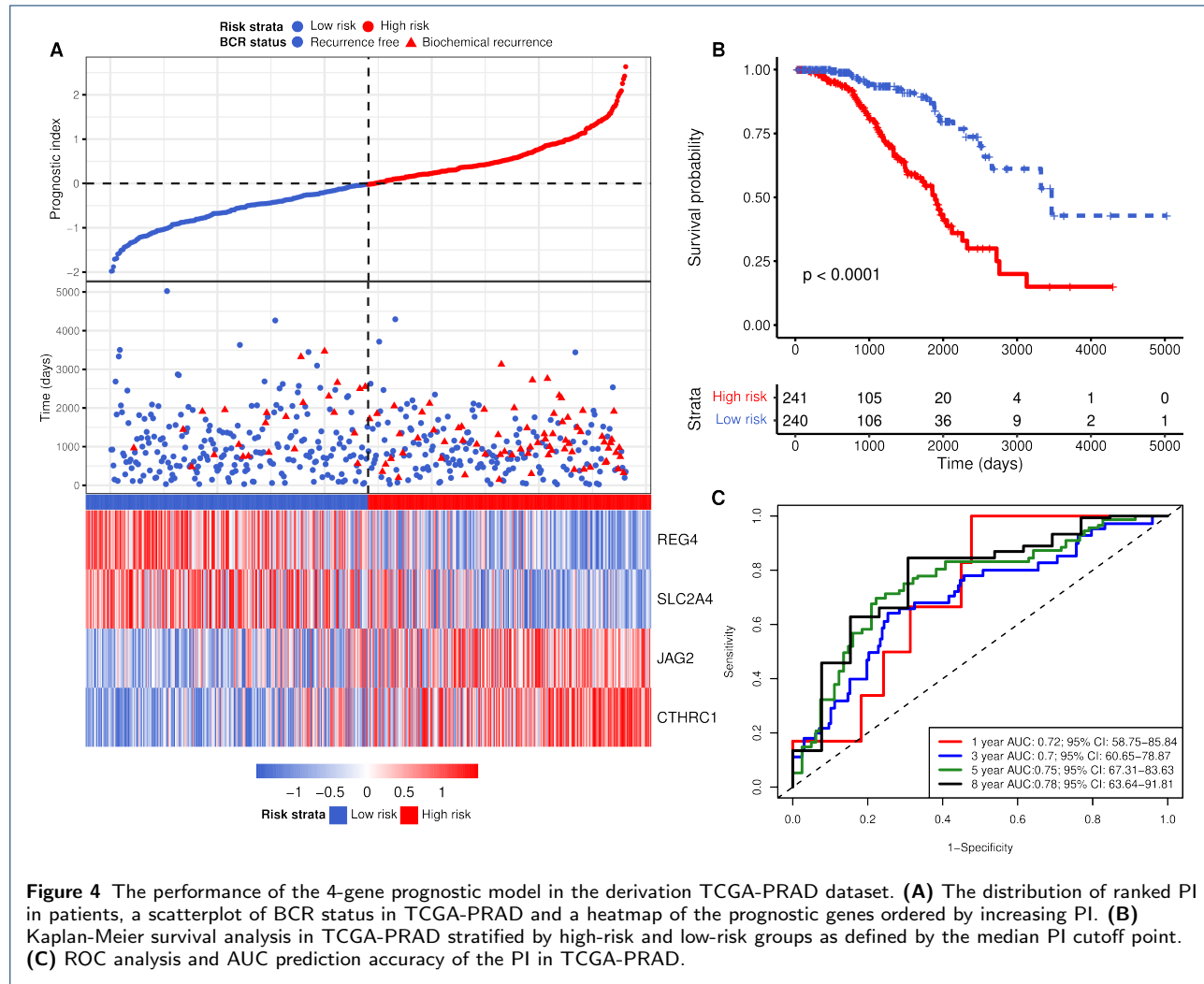
fined by the median prognostic index value, were plotted to provide informal evidence of discrimination. 5) Hazard ratios between risk groups were computed in the validation and derivation dataset. Ideally, the hazard ratio in the derivation dataset is well maintained in the validation dataset and remains statistically significant. 6) ROC analysis revealed the overall predictive accuracy of the model via AUC. All external datasets were processed in an identical manner to the derivation dataset as previously described.

Estimation of infiltrating cells and tumour purity

The Estimation of STromal and Immune cells in Malignant Tumours using Expression data (ESTIMATE) was obtained for TCGA-PRAD samples via the [ESTIMATE website](#) [73]. ESTIMATE provides insights into the presence of stroma in tumor tissue, the infiltration of immune cells in tumor tissue and the overall tumor purity via stromal, immune and ESTIMATE scores, respectively. Microenvironment Cell Populations-counter (MCP-counter) was applied to TCGA-PRAD samples to quantify the abundance of CD3⁺ T cells, CD8⁺ T cells, cytotoxic lymphocytes,

Table 5 Evaluation of the derivation dataset and the validation datasets used in the study.

	Calibration slope			Chi-squared		Harrell's C	High risk stratum		
	coef	(95% CI)	P-value	χ^2_5	P-value		Hazard ratio	(95% CI)	P-value
TCGA-PRAD	1.00	(0.73, 1.26)	<0.001	0	1	0.71	3.78	(2.37, 6.03)	<0.001
DKFZ	1.23	(0.81, 1.66)	<0.001	6.03	0.644	0.79	4.79	(1.78, 12.86)	0.002
Taylor	1.04	(0.20, 1.89)	0.015	5.8	0.67	0.63	2.18	(0.99, 4.77)	0.052
GSE54460	0.71	(0.31, 1.11)	<0.001	6.86	0.55	0.69	3.51	(1.88, 6.56)	<0.001
CPC	0.64	(0.16, 1.11)	0.009	3.79	0.875	0.67	1.99	(1.01, 3.89)	0.045
Stockholm	0.62	(0.23, 1.01)	0.002	4.26	0.833	0.65	2.27	(1.23, 4.16)	0.008
Belfast	0.34	(0.00, 0.68)	0.051	18.27	0.019	0.61	1.81	(1.06, 3.09)	0.031



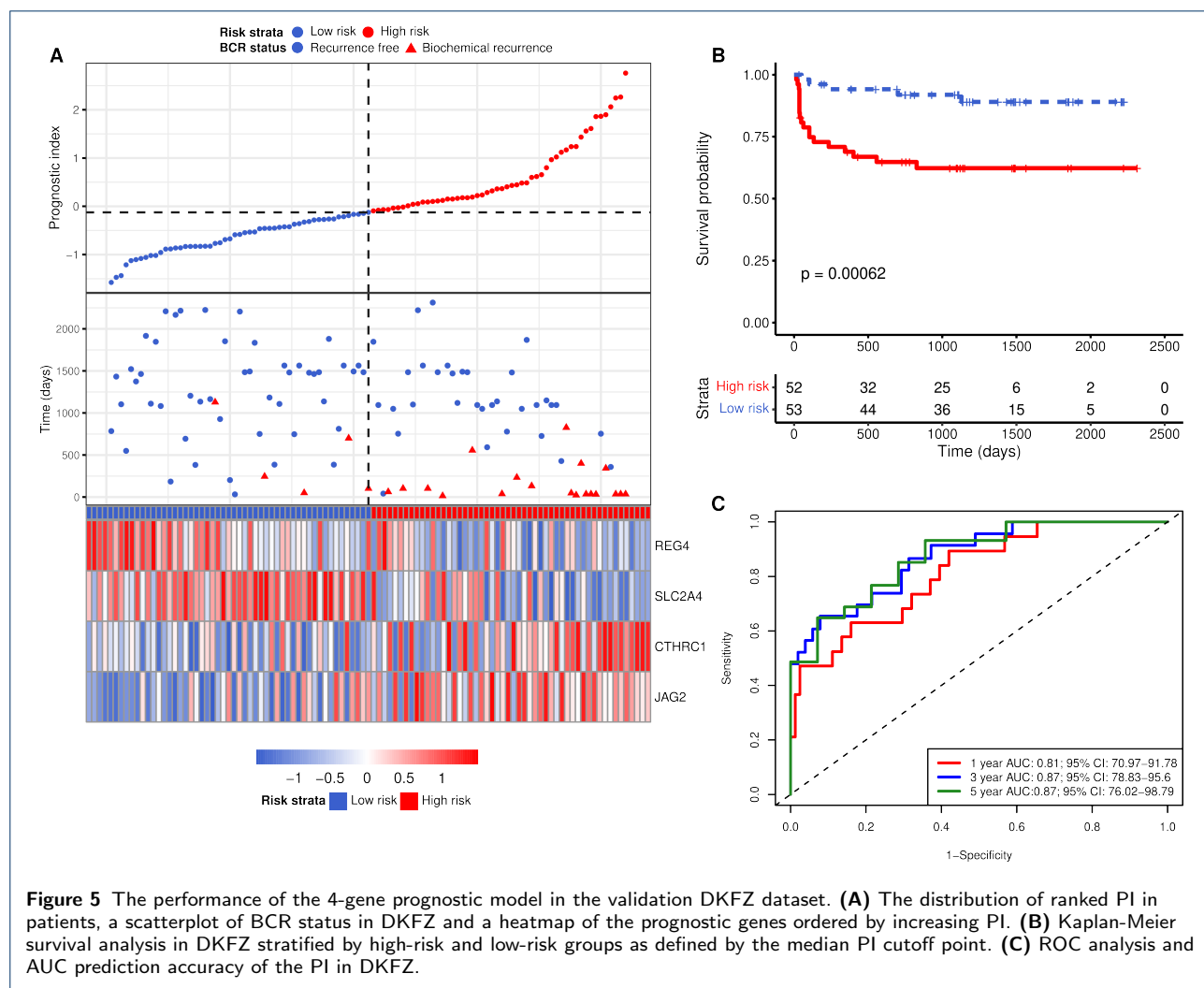
NK cells, B lymphocytes (B lineage), cells originating from monocytes (monocytic lineage), myeloid dendritic cells, neutrophils, as well as endothelial cells and fibroblasts. Finally, 28 Tumor-Immune System Interaction (TISI) gene sets were downloaded from [TISIDB](#). Single-sample GSEA was performed using the GSVA R package [74] to derive per-sample enrichment scores. Student's T-test was performed to delineate differences in immune infiltration and expression in the high-risk

and low-risk strata for each of ESTIMATE, MCP-counter and TISIDB scores.

Results

Identification of the ceRNA network

Datasets downloaded in the study were subject to differential expression analysis and the downstream intersection of results to derive a common signature in enzalutamide resistance and prostate cancer. The

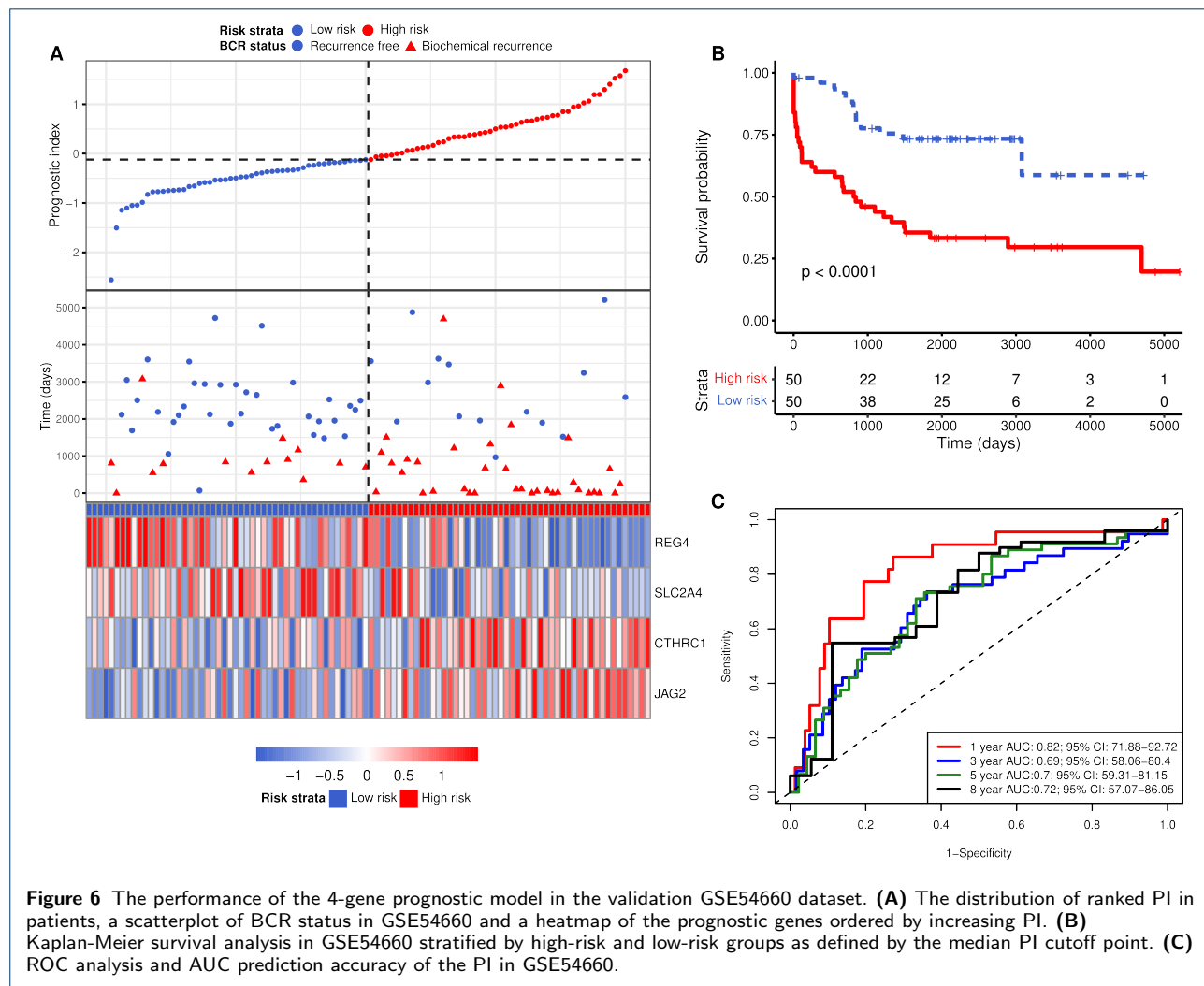


contrasts used in each analysis and the summary of their results are provided in Table 3. Differential circRNA expression analysis revealed 279 DE-circRNAs (174 up-regulated, 105 down-regulated). Target prediction of circRNAs using the CircBase and CDSC databases returned 2754 predicted circRNA-miRNA pairs which were subset using the results of differentially expressed miRNAs (16 up-regulated, 26 down-regulated) to produce a final set of 41 DE-miRNAs (Figure 1A). TargetScan, miRNet, miRTarBase and miRBase returned 15712 miRNA-mRNA target predictions based on the input 41 DE-miRNAs. Predictions were intersected using 368 DE-mRNAs returned by differential gene expression analysis (196 up-regulated, 172 down-regulated), resulting in a set of 320 DE-mRNAs (Figure 1B). The preliminary ceRNA network consisting of 278 circRNAs, 41 miRNAs and 320 mRNAs was subject to filtering based on the ceRNA hypothesis to generate a ceRNA network consisting of 141 circRNAs, 40 miRNAs and 256 mRNAs.

Functional analysis of DE-mRNAs using pathfindR annotated 29, 33 and 57 GO, KEGG and Reactome pathways, respectively (Figure 2). Pathways involved in the epithelial-mesenchymal transition (EMT) were enriched in addition to CASP8 inhibition, protein ubiquitination and SUMOylation pathways contributing to the survival and proliferation of cancer cells within the tumor microenvironment. DARPP-32 and FCER1-mediated Ca²⁺ mobilization may contribute to the progression of prostate cancer and the acquisition of a chemotherapeutic drug-resistant phenotype.

Prognostic model development

The 256 DE-mRNAs returned by the enzalutamide ceRNA network were used to derive a model predictive of BCR in PCa. Univariate Cox regression analysis initially identified 24 genes associated with BCR (Supplementary file 1), of which 4 were discarded for violating the proportional hazard assumptions (Supplementary figure 1). A multivariate Cox regression



model was fit for the remaining 20 genes and via backward selection, a 7 gene signature was identified (Supplementary file 2). After applying a filter of $P \leq 0.05$ to the 7 genes, we arrived at a 4 gene signature comprising *REG4*, *SLC2A4*, *CTHRC1* and *JAG2*. *REG4* and *SLC2A4* are considered protective against BCR, whilst *CTHRC1* and *JAG2* increase the risk of BRC in PCa patients (Table 4, Supplementary file 3).

Evaluation of the prognostic model

The prognostic model was firstly evaluated in the derivation TCGA-PRAD dataset by stratifying patients into high-risk and low-risk strata using the median prognostic index, resulting in 241 and 240 patients with 74 and 21 BCR events in each stratum, respectively. Kaplan-Meier survival analysis and a log-rank test revealed high-risk groups are significantly associated with worse BCR prognosis ($HR=3.78$, $CI=(2.37, 6.03)$, $P=<0.001$) (Table 5, Figure 4B).

ROC analysis of the prognostic index as a marker revealed an AUC of 1-year (0.72), 3-years (0.7), 5-years (0.75) and 8-years (0.78) indicating the prognostic index can predict BCR with reasonable accuracy (Figure 4C).

The model was further evaluated in six external datasets, in some cases outperforming the statistics generated by the derivation dataset (Table 5) highlighting the robustness of the gene signature in predicting BCR. Of particular note is the performance of the model in the DKFZ and GSE54660 validation datasets. The calibration slope and Harrell's c-index in the DKFZ dataset suggest the model has enhanced classification performance, confirmed by a high AUC of 1-year (0.81), 3-years (0.87) and 5-years (0.87) (Figure 5C). The Hazard ratio generated by the DKFZ dataset for the high-risk stratum ($HR=4.79$, $CI=(1.78, 12.86)$, $P=0.002$) and Kaplan-Meier plots coupled with a log-rank test ($P=0.00062$, Figure 5B) indicate patient stratification using the prognostic index was sta-

Table 6 Results of univariate and multivariate Cox regression analysis with clinical features.

Variable	Univariate Cox			Multivariate Cox		
	Hazard Ratio	(95% CI)	P-value	Hazard Ratio	(95% CI)	P-value
Age						
<56	Reference					
≥56	2.11	(1.19, 3.73)	0.010	2.06	(1.11, 3.81)	0.02
PSA						
<10ng/ml	(Reference)					
10-20ng/ml	1.33	(0.82, 2.15)	0.248	0.99	(0.60, 1.63)	0.97
>20mg/ml	1.38	(0.77, 2.49)	0.284	0.76	(0.40, 1.44)	0.40
Gleason Score						
Gleason 6 or lower	Reference					
Gleason 7	4.46	(0.60, 32.84)	0.143	3.54	(0.48, 26.34)	0.22
Gleason 8,9,10	13.78	(1.91 99.29)	0.009	4.92	(0.66, 36.81)	0.12
Pathologic T						
T2	Reference					
T3	4.46	(2.42, 8.21)	<0.001	2.22	(1.17, 4.24)	0.02
T4	2.45	(0.55, 11.04)	0.242	0.69	(0.14, 3.33)	0.65
Pathologic N						
N0	Reference					
N1	2.33	(1.49, 3.64)	<0.001	1.04	(0.63, 1.73)	0.87
Clinical M						
M0	Reference					
M1	7.37	(1.01, 53.80)	0.049	1.68	(0.21, 13.57)	0.63
Resection status						
R0	Reference					
R1/R2	2.11	(1.40, 3.19)	<0.001	1.73	(1.08, 2.79)	0.02
RX	1.00	(0.31, 3.22)	0.999	0.55	(0.17, 1.84)	0.33
Prognostic index	2.72	(2.09, 3.54)	<0.001	2.21	(1.62, 3.01)	<0.001

tistically significant and useful in predicting worse BCR prognosis. The GSE54660 dataset largely preserved the derivation datasets Harrel's c-index and Hazard ratios ($C=0.69$, $HR=3.51$, $CI=(1.88, 6.56)$, $P=<0.001$) suggesting the predictive model fit well to the GSE4660 validation dataset (Figure 6B). The predictive accuracy in the GSE54660 dataset was acceptable, with an AUC of 1-year (0.82), 3-years (0.69), 5-years (0.7), and 8-years (0.72) (Figure 6C). In the remaining validation datasets, the prognostic model was indeed useful in creating statistically significant strata via the prognostic index, albeit to a lesser degree as revealed by the logrank test (Taylor $P=0.047$, CPC $P=0.041$, Stockholm $P=0.0067$, Belfast $P=0.028$, Supplementary figure 2,3,4,5). Taken together, we demonstrate the utility of the 4-gene prognostic model in predicting BCR in various datasets.

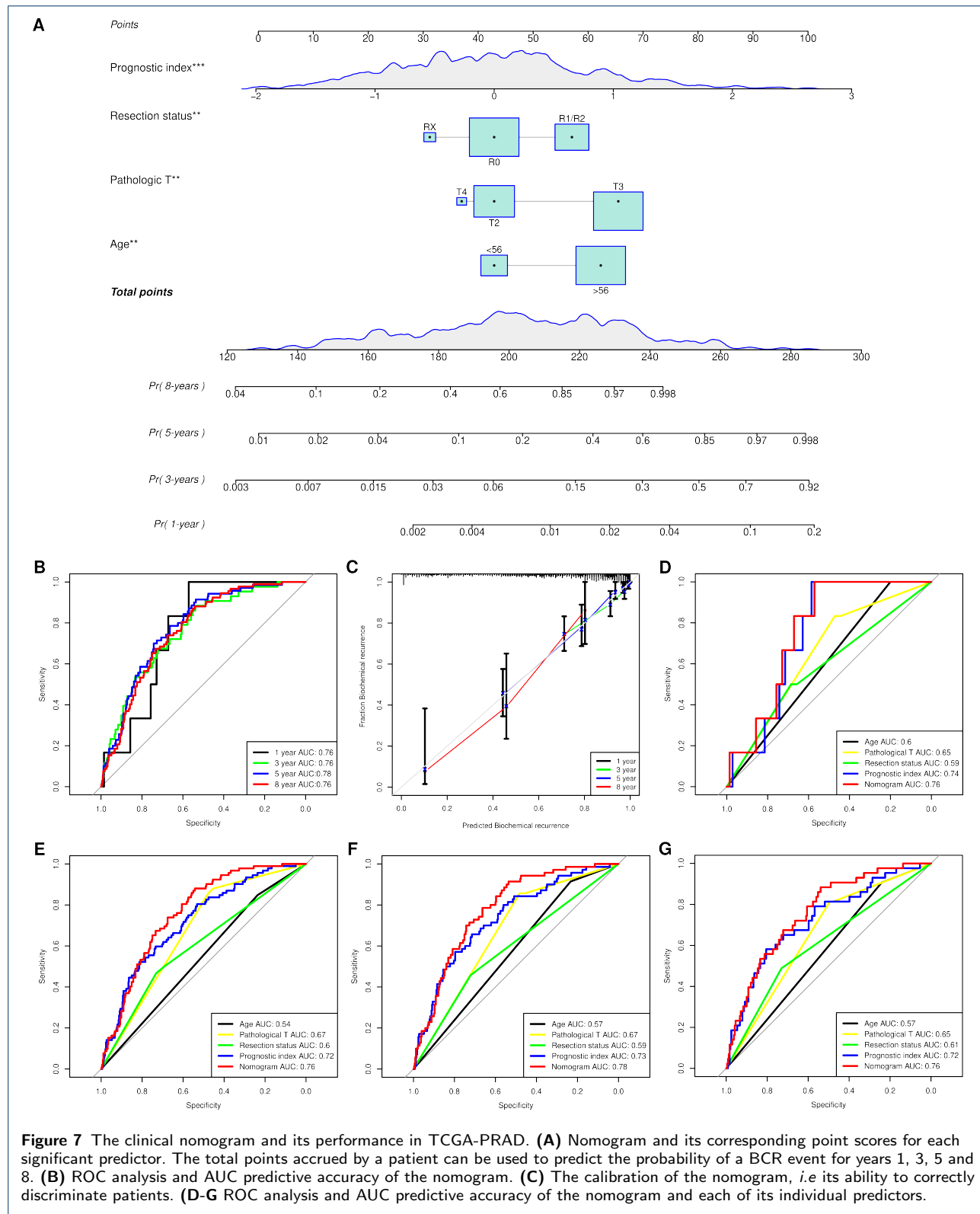
Combined clinical nomogram

The derivation dataset PI and clinical covariates age, PSA, Gleason score, pathologic T, pathologic N, clinical M and surgical resection status were incorporated in a univariate and multivariate Cox model (Table 6). Encouragingly, the PI was independent of other clinical covariates in the multivariate model ($HR=2.21$, $CI=(1.62, 3.01)$, $P=<0.001$). The covariates age, pathologic T and resection status remained significant in the multivariate model and were included in the final clinical model. A Harrell's c-index of 0.71

indicated good consistency when including clinical covariates. Furthermore, AUC scores of 1-year (0.76), 3-years (0.76), 5-years (0.78) and 8-years (0.76) (Figure 7B) in the clinical model outperformed each of the individual predictors in the clinical model (Figure 7D-G) and the prediction accuracy of the derivation model for years 1, 3 and 5 (Figure 5C). Investigating the calibration plot for 8-years in the clinical model reveals the clinical model was over-optimistic in predicting BCR (Figure 7C).

Immune TME of high-risk and low-risk groups

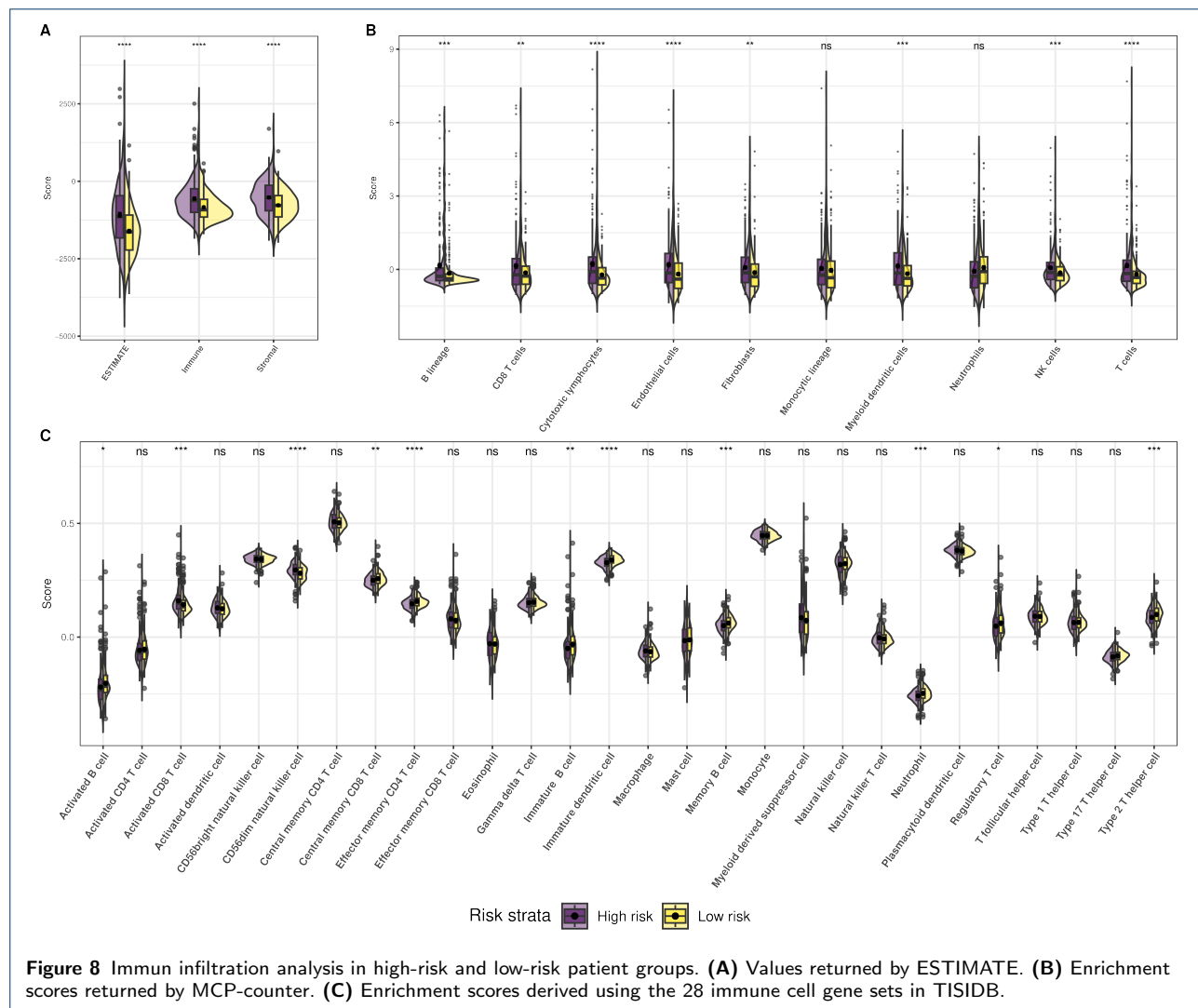
ESTIMATE, MCP-counter and TISIDB immune gene set analysis was performed to elucidate differential immune features in each strata. In the high-risk group, ESTIMATE revealed higher presence of stromal cells, immune cells and tumor purity ($P\leq 0.05$, Figure 8A). MCP-counter results were all enriched in high-risk patients, except for macrophages and neutrophils which displayed no significant differences between the two strata (Figure 8B). Finally, the 28 TISIDB immune gene sets were analysed using ssGSEA. Activated/immature/memory B cells, central/effectector memory CD8 T cells, immature dendritic cells, neutrophils, regulatory T cells and type 2 T helper cells were all enriched in low-risk patients. Activated CD8 T cells and CD65dim natural killer cells were enriched in high-risk patients (Figure 8C).



Pathways associated with prognostic index

To identify functional pathways associated with PI, ssGSEA was performed on KEGG pathways to derive

per-patient enrichment scores used as input for subsequent correlation analysis. Pearsons correlation coef-



ficient >0.25 and $P \leq 0.05$ was deemed significant, resulting in 35 pathways of which 8 were positively correlated with prognostic index, and 27 displayed negative correlation (Figure 9). The majority of pathways related to prognostic index stem from immune responses to pathogen-associated molecular patterns (PAMPs) and damage-associated molecular patterns (DAMPs) suggesting elevated immune activity in high-risk patients. Interestingly, pathways correlated with low-risk patients involved amino acid and fatty acid metabolism hinting at elevated levels of oxidative phosphorylation which when down-regulated, correlates with poor clinical outcomes in several cancer types and the presence of epithelial-to-mesenchymal (EMT) signature [75].

Discussion

We present a 4-gene prognostic signature based on the integration of circRNA-miRNA-mRNA prostate

cancer and enzalutamide resistance datasets to gain insights into the mechanism of biochemical recurrence. The 4-gene signature produced a prognostic index from the derivation TCGA-PRAD dataset that effectively stratified patients into high-risk and low-risk strata exhibiting robust performance in the Belfast, CPC, DKFZ, GSE54460, Taylor and Stockholm PCa datasets. Whilst previous studies have generated circRNA-miRNA-mRNA regulatory networks in prostate cancer [76], to the best of our knowledge, this work represents the first study that provides a prognostic signature and corresponding prognostic index for use in external validation datasets. We also demonstrate the independence of the prognostic index in relation to clinical features, deriving a clinical nomogram that outperforms the performance of the prognostic index in standalone use. Finally, we elucidate the differential immune features in high-risk and low-risk groups via immune infiltration analysis

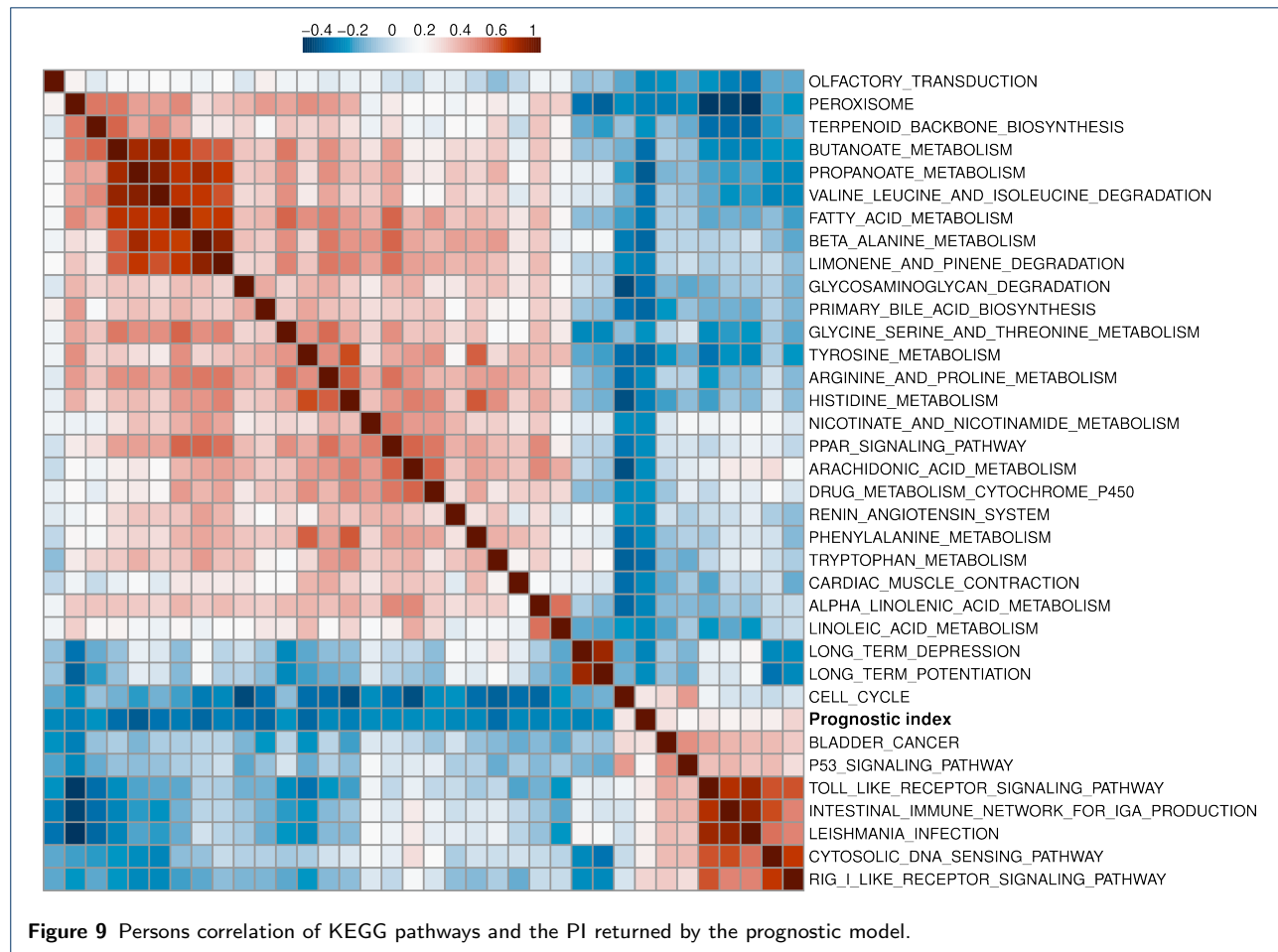


Figure 9 Persons correlation of KEGG pathways and the PI returned by the prognostic model.

to identify potential immune biomarkers in prostate cancer.

Through literature searches, we further assessed the prognostic ceRNA network (Figure 3). hsa-circ-0000442, expressed by the *MED13L* gene, has been demonstrated to exert a tumor-suppressing role in breast cancer [77]. In our analysis, we observed up-regulation of hsa-circ-0000442 which is predicted to sequester hsa-miR-26a-5p thereby preventing the post-transcriptional degradation of *REG4*. Our prognostic signature indicates *REG4* is protective against biochemical recurrence hence up-regulation of the hsa-circ-0000442 circular transcript may be linked with improved disease-free survival. hsa-circ-0001258 (parent gene *PPP6R2*) was found to be down-regulated in osteosarcoma chemoresistance groups compared to chemosensitive groups. Transfection of osteosarcoma cells with hsa-circ-0001258 expression vector revealed suppressed doxorubicin resistance [78]. In our study we report similar fold change direction of hsa-circ-0001258 in enzalutamide-resistant cells, hinting that the circRNA may play a role in drug resistance. The miRNA

hsa-miR-106a-5p is highly expressed in prostate cancer cells vs normal and high grade (Gleason >7) tumors vs low-grade tumours and is associated with poor disease-free survival [79]. Despite our study demonstrating similar expression levels for hsa-miR-106a-5p, its predicted role in degrading *SLC2A4* transcripts was shown to be a protective factor against biochemical recurrence. Our study also demonstrated the down-regulation of hsa-miR-26a-5p, confirmed to be significantly decreased in prostate cancer tissues compared with controls in prostate cancer cell lines VCaP, 22RV1, LNCaP, and DU-145 [80].

JAG2 (Jagged Canonical Notch Ligand 2) is a member of NOTCH ligands involved in the NOTCH signalling pathway. *JAG2* has been implicated with tumor progression in bladder cancer [81], lung cancer [82] and colorectal cancer [83] however, due to the pleiotropic nature of *JAG2* in cells, its value as a prognostic marker is largely cancer-specific. Whilst prostate cancer patients with Gleason scores ≥ 8 exhibited up-regulation of *JAG2* [84], our results contradict these findings; *JAG2* was down-regulated in TCGA-PRAD and enzalutamide-resistant cells. *CTHRC1*

(Collagen Triple Helix Repeat Containing 1) knockdown suppressed prostate cancer cell proliferation, migration and invasion. The authors also demonstrated that *CTHRC1* was negatively regulated by miR-30e-5p [85]. In our study, we show that up-regulation of hsa-circ-0004291, hsa-circ-0035301, hsa-circ-0001278, hsa-circ-0007178 potentially inhibits miR-30c-5p, resulting in up-regulation of *CTHRC1*. The interplay between the miR-30 family and *CTHRC1* therefore warrants further investigation. Studies of *REG4* (Regenerating Family Member 4) generally agree with our findings: utility as an independent prognostic marker of relapse after radical prostatectomy [86] and similarly elevated expression in tumour prostate cancer cells vs. normal [87]. Our study found that *SLC2A4* (Solute Carrier Family 2 (Facilitated Glucose Transporter), Member 4 - commonly denoted as *GLUT4*) was downregulated in prostate cancer and enzalutamide resistance, exhibiting a protective effect against BCR. Of note, *SLC2A4* was downregulated in high-risk patients compared to low-risk. Metformin has been shown to induce *SLC2A4* translocation to the cell surface [88], enhancing the effects of the antiandrogen bicalutamide and enzalutamide in CRPC patients [89–91]. We therefore propose downregulation of *SLC2A4* may serve as a prognostic marker in prostate cancer patients.

Conclusions

To conclude, this study leveraged existing and novel circRNA-miRNA-mRNA datasets to derive a prognostic signature with robust performance in multiple datasets. It represents the first work deriving a prognostic gene signature based on the competing endogenous RNA network hypothesis involving circRNAs. In addition to the prognostic value of the signature, the 4 genes emerged as candidates for further understanding the mechanism of biochemical recurrence in prostate cancer.

Additional Files

Pilib - hyperlinks to the documents are temporary placeholders.

Abbreviations

To do

Acknowledgements

We thank Dr. Marvin Lim and Dr. Elaine Kenny for the preparation and sequencing of the in-house LNCaP cell lines.

Authors' contributions

B.D. designed and performed the analysis and drafted the manuscript. P.O.B. and S.P.F. supervised the work, gave feedback, and revised the manuscript.

Availability of data and materials

The code used to perform the analysis is freely available at https://github.com/BarryDigby/pca_network. Due to file size constraints, files $\geq 20\text{MB}$ used in the analysis are unavailable. The authors can provide these files upon reasonable request.

Funding

Open access and PhD scholarship funding for B.D. provided by Science Foundation Ireland, grant number 18/CRT/6214. No funding body played any role in the design of the study and collection, analysis, interpretation of data or in writing the manuscript.

Competing interests

The authors declare that they have no competing interests.

Ethics approval and consent to participate

Not applicable.

Author details

¹School of Mathematical and Statistical Sciences, University of Galway, Galway, Ireland. ²Department of Histopathology and Morbid Anatomy, Trinity Translational Medicine Institute, Dublin, Ireland.

References

1. Sung, H., Ferlay, J., Siegel, R.L., Laversanne, M., Soerjomataram, I., Jemal, A., Bray, F.: Global Cancer Statistics 2020: GLOBOCAN Estimates of Incidence and Mortality Worldwide for 36 Cancers in 185 Countries. CA Cancer J. Clin. **71**(3), 209–249 (2021). doi:[10.3322/caac.21660](https://doi.org/10.3322/caac.21660)
2. Lim, M.C.J., Baird, A.-M., Aird, J., Greene, J., Kapoor, D., Gray, S.G., McDermott, R., Finn, S.P.: RNAs as Candidate Diagnostic and Prognostic Markers of Prostate Cancer—From Cell Line Models to Liquid Biopsies. Diagnostics **8**(3), 60 (2018). doi:[10.3390/diagnostics8030060](https://doi.org/10.3390/diagnostics8030060)
3. Cornford, P., Bellmunt, J., Bolla, M., Briers, E., De Santis, M., Gross, T., Henry, A.M., Joniau, S., Lam, T.B., Mason, M.D., van der Poel, H.G., van der Kwast, T.H., Rouvière, O., Wiegel, T., Mottet, N.: EAU-ESTRO-SIOG Guidelines on Prostate Cancer. Part II: Treatment of Relapsing, Metastatic, and Castration-Resistant Prostate Cancer. Eur. Urol. **71**(4), 630–642 (2017). doi:[10.1016/j.eururo.2016.08.002](https://doi.org/10.1016/j.eururo.2016.08.002)
4. Scher, H.I., Fizazi, K., Saad, F., Taplin, M.-E., Sternberg, C.N., Miller, K., de Wit, R., Mulders, P., Chi, K.N., Shore, N.D., Armstrong, A.J., Flraig, T.W., Fléchon, A., Mainwaring, P., Fleming, M., Hainsworth, J.D., Hirmand, M., Selby, B., Seely, L., de Bono, J.S., Investigators, A., Alasino, C., Bella, S., Carraro, S., Geist, M., Abdi, E., Begbie, S., Briscoe, K., Davis, I., Dowling, A., Ganju, V., Gurney, H., Hovey, E., Ng, S., Nottage, M., Rosenthal, M., Stockler, M., Tan, T.H., Wong, S., Young, R., Krainer, M., Loidl, W., Machiels, J.P., Mebis, J., Renard, V., Dumez, H., Van Aelst, F., Werbrouck, P., Ellard, S., Joshua, A., Karakiewicz, P., Lacombe, L., Lattouf, J.B., Michels, J., Mukherjee, S., Ruether, D., Venner, P., Winquist, E., Wood, L., Aren, O., Gonzalez, P., Pastor, P., Baumgaertner, I., Beuzeboc, P., Bompas, E., Boyle, H., Colombel, M., Delva, R., Eymard, J.C., Gravis, G., Guillot, A., Houédé, N., Joly, F., Kaphan, R., Loriot, Y., Ouard, S., Priou, F., Tartas, S., Theodore, C., Tourani, J.-M., Voog, E., Bögemann, M., Hadachik, B., Hammerer, P., Heidenreich, A., Holzer, W., Merseburger, A., Stenzl, A., Steuber, T., Suttmann, H., Trojan, L., Wirth, M., Cerbone, L., Conte, P., Passalacqua, R., Tucci, M., Gerritsen, W., Jassem, J., Kalinka-Warzocha, E., Olubie, J., De Bruyne, R., Malan, J., Vorobiof, D., Bellmunt, J., Carles, J., Durán, I., Font, A., Gil-Bazo, I., Maroto, J.P., Bahl, A., Choudhury, A., Hoskin, P., James, N., Jones, R., Mazhar, D., O'Sullivan, J., Payne, H., Pedley, I., Protheroe, A., Waxman, J., Zivi, A., Alexander, B., Appleman, L., Aragon-Ching, J., Arrowsmith, E., Assikis, V., Beer, T., Berry, W., Bolger, G., Bryce, A., Bubley, G., Chatta, G., Denmeade, S., Deshpande, H., Dorff, T., Galsky, M., George, D., Giudice, R., Glode, M., Golshayan, A.-R., Goodman, O., Graff, J., Green, L., Green, R., Haas, N., Higano, C., Hutson, T., Kohli, M., Liu, G., May, J., Mendelson, D., Picus, J., Pili, R., Posadas, E., Redfern, C., Rettig, M., Ryan, C., Scholz, M., Sharifi, N., Sosman, J., Srinivas, S., Tagawa, S., Twardowski, P., Vaishampayan, U., Wong, Y.-N.: Increased survival with enzalutamide in prostate cancer after chemotherapy. N. Engl. J. Med. **367**(13), 1187–1197 (2012). doi:[10.1056/NEJMoa1207506](https://doi.org/10.1056/NEJMoa1207506). 2289453
5. Yang, Z., Qu, C.-B., Zhang, Y., Zhang, W.-F., Wang, D.-D., Gao, C.-C., Ma, L., Chen, J.-S., Liu, K.-L., Zheng, B., Zhang, X.-H., Zhang, M.-L., Wang, X.-L., Wen, J.-K., Li, W.: Dysregulation of p53-RBM25-mediated circAMOTL1L biogenesis contributes to prostate cancer progression through the

- circAMOTL1L-miR-193a-5p-Pcdha pathway. *Oncogene* **38**, 2516–2532 (2019). doi:[10.1038/s41388-018-0602-8](https://doi.org/10.1038/s41388-018-0602-8)
6. Taylor, B.S., Schultz, N., Hieronymus, H., Gopalan, A., Xiao, Y., Carver, B.S., Arora, V.K., Kaushik, P., Cerami, E., Reva, B., Antipin, Y., Mitisades, N., Landers, T., Dolgalev, I., Major, J.E., Wilson, M., Soccia, N.D., Lash, A.E., Heguy, A., Eastham, J.A., Scher, H.I., Reuter, V.E., Scardino, P.T., Sander, C., Sawyers, C.L., Gerald, W.L.: Integrative genomic profiling of human prostate cancer. *Cancer Cell* **18**(1), 11–22 (2010). doi:[10.1016/j.ccr.2010.05.026](https://doi.org/10.1016/j.ccr.2010.05.026). [20579941](https://doi.org/10.2579941)
 7. Wach, S., Nolte, E., Szczyrba, J., Stöhr, R., Hartmann, A., Ørntoft, T., Dyrskjøt, L., Eltze, E., Wieland, W., Keck, B., Ekici, A.B., Grässer, F., Wullich, B.: MicroRNA profiles of prostate carcinoma detected by multiplatform microRNA screening. *Int. J. Cancer* **130**(3), 611–621 (2012). doi:[10.1002/ijc.26064](https://doi.org/10.1002/ijc.26064). [21400514](https://doi.org/21400514)
 8. Lin, P.-C., Chiu, Y.-L., Banerjee, S., Park, K., Mosquera, J.M., Giannopoulos, E., Alves, P., Tewari, A.K., Gerstein, M.B., Beltran, H., Melnick, A.M., Elemento, O., Demichelis, F., Rubin, M.A.: Epigenetic repression of miR-31 disrupts androgen receptor homeostasis and contributes to prostate cancer progression. *Cancer Res.* **73**(3), 1232–1244 (2013). doi:[10.1158/0008-5472.CAN-12-2968](https://doi.org/10.1158/0008-5472.CAN-12-2968). [23233736](https://doi.org/23233736)
 9. Casanova-Salas, I., Rubio-Briones, J., Calatrava, A., Mancarella, C., Masiá, E., Casanova, J., Fernández-Serra, A., Rubio, L., Ramírez-Backhaus, M., Armiñán, A., Domínguez-Escríg, J., Martínez, F., García-Casado, Z., Scotlandi, K., Vicent, M.J., López-Guerrero, J.A.: Identification of miR-187 and miR-182 as biomarkers of early diagnosis and prognosis in patients with prostate cancer treated with radical prostatectomy. *J. Urol.* **192**(1), 252–259 (2014). doi:[10.1016/j.juro.2014.01.107](https://doi.org/10.1016/j.juro.2014.01.107). [24518785](https://doi.org/24518785)
 10. Leite, K.R.M., Reis, S.T., Viana, N., Morais, D.R., Moura, C.M., Silva, I.A., Pontes, J. Jr., Katz, B., Srougi, M.: Controlling RECK miR21 Promotes Tumor Cell Invasion and Is Related to Biochemical Recurrence in Prostate Cancer. *J. Cancer* **6**(3), 292–301 (2015). doi:[10.7150/jca.11038](https://doi.org/10.7150/jca.11038). [25663948](https://doi.org/25663948)
 11. Grossman, R.L., Heath, A.P., Ferretti, V., Varmus, H.E., Lowy, D.R., Kibbe, W.A., Staudt, L.M.: Toward a Shared Vision for Cancer Genomic Data. *N. Engl. J. Med.* **375**(12), 1109–1112 (2016). doi:[10.1056/NEJMp1607591](https://doi.org/10.1056/NEJMp1607591). [27653561](https://doi.org/27653561)
 12. Greene, J., Baird, A.-M., Casey, O., Brady, L., Blackshields, G., Lim, M., O'Brien, O., Gray, S.G., McDermott, R., Finn, S.P.: Circular RNAs are differentially expressed in prostate cancer and are potentially associated with resistance to enzalutamide. *Sci. Rep.* **9**(1), 10739 (2019). doi:[10.1038/s41598-019-47189-2](https://doi.org/10.1038/s41598-019-47189-2). [31341219](https://doi.org/31341219)
 13. Lim, M.C.J., Baird, A.-M., Greene, J., McNevin, C., Ronan, K., Podlesnyi, P., Sheils, O., Gray, S.G., McDermott, R.S., Finn, S.P.: hsa_circ_0001275 Is One of a Number of circRNAs Dysregulated in Enzalutamide Resistant Prostate Cancer and Confers Enzalutamide Resistance In Vitro. *Cancers* **13**(24), 6383 (2021). doi:[10.3390/cancers13246383](https://doi.org/10.3390/cancers13246383). [34945002](https://doi.org/34945002)
 14. Kaylyn D. Tousignant, #., Rockstroh, A., Poad, B.L.J., Talebi, A., Young, R.S.E., Fard, A.T., Gupta, R., Zang, T., Wang, C., Lehman, M.L., Swinnen, J.V., Blanksby, S.J., Nelson, C.C., Martin C. Sadowski, #.: Therapy-induced lipid uptake and remodeling underpin ferroptosis hypersensitivity in prostate cancer. *Cancer Metab.* **8**, 11 (2020). doi:[10.1186/s40170-020-00217-6](https://doi.org/10.1186/s40170-020-00217-6). [32577235](https://doi.org/32577235)
 15. Kregel, S., Chen, J.L., Tom, W., Krishnan, V., Kach, J., Brechka, H., Fessenden, T.B., Isikbay, M., Paner, G.P., Szmulewitz, R.Z., Griend, D.J.V.: Acquired resistance to the second-generation androgen receptor antagonist enzalutamide in castration-resistant prostate cancer. *Oncotarget* **7**(18), 26259–26274 (2016). doi:[10.18632/oncotarget.8456](https://doi.org/10.18632/oncotarget.8456). [27036029](https://doi.org/27036029)
 16. Li, Q., Deng, Q., Chao, H.-P., Liu, X., Lu, Y., Lin, K., Liu, B., Tang, G.W., Zhang, D., Tracz, A., Jeter, C., Rycaj, K., Calhoun-Davis, T., Huang, J., Rubin, M.A., Beltran, H., Shen, J., Chatta, G., Puzanov, I., Mohler, J.L., Wang, J., Zhao, R., Kirk, J., Chen, X., Tang, D.G.: Linking prostate cancer cell AR heterogeneity to distinct castration and enzalutamide responses. *Nat. Commun.* **9**(1), 3600 (2018). doi:[10.1038/s41467-018-06067-7](https://doi.org/10.1038/s41467-018-06067-7). [30190514](https://doi.org/30190514)
 17. Lopez, J.P., Diallo, A., Cruceanu, C., Fiori, L.M., Laboissiere, S., Guillet, I., Fontaine, J., Ragoussis, J., Benes, V., Turecki, G., Ernst, C.: Biomarker discovery: quantification of microRNAs and other small non-coding RNAs using next generation sequencing. *BMC Med.* **Genomics** **8**(1), 1–18 (2015). doi:[10.1186/s12920-015-0109-x](https://doi.org/10.1186/s12920-015-0109-x)
 18. Nimse, S.B., Sonawane, M.D., Song, K.-S., Kim, T.: Biomarker detection technologies and future directions. *Analyst* **141**(3), 740–755 (2016). doi:[10.1039/C5AN01790D](https://doi.org/10.1039/C5AN01790D)
 19. Xi, X., Li, T., Huang, Y., Sun, J., Zhu, Y., Yang, Y., Lu, Z.J.: RNA Biomarkers: Frontier of Precision Medicine for Cancer. *Non-Coding RNA* **3**(1) (2017). doi:[10.3390/ncrna3010009](https://doi.org/10.3390/ncrna3010009)
 20. Consortium, T.E.P.: An integrated encyclopedia of DNA elements in the human genome. *Nature Publishing Group*. [Online; accessed 20. Sep. 2023] (2012). doi:[10.1038/nature11247](https://doi.org/10.1038/nature11247)
 21. Djebali, S., Davis, C.A., Merkel, A., Dobin, A., Lassmann, T., Mortazavi, A., Tanzer, A., Lagarde, J., Lin, W., Schlesinger, F., Xue, C., Marinov, G.K., Khatushi, J., Williams, B.A., Zaleski, C., Rozowsky, J., Röder, M., Kokocinski, F., Abdelhamid, R.F., Alioto, T., Antoshechkin, I., Baer, M.T., Bar, N.S., Batut, P., Bell, K., Bell, I., Chakrabortty, S., Chen, X., Chrast, J., Curado, J., Derrien, T., Drenkow, J., Dumais, E., Dumais, J., Duttagupta, R., Falconet, E., Fastuca, M., Fejes-Toth, K., Ferreira, P., Foissac, S., Fullwood, M.J., Gao, H., Gonzalez, D., Gordon, A., Gunawardena, H., Howald, C., Jha, S., Johnson, R., Kapranov, P., King, B., Kingswood, C., Luo, O.J., Park, E., Persaud, K., Preall, J.B., Ribeca, P., Risk, B., Robyr, D., Sammeth, M., Schaffer, L., See, L.-H., Shahab, A., Skancke, J., Suzuki, A.M., Takahashi, H., Tilgner, H., Trout, D., Walters, N., Wang, H., Wrobel, J., Yu, Y., Ruan, X., Hayashizaki, Y., Harrow, J., Gerstein, M., Hubbard, T., Raymond, A., Antonarakis, S.E., Hannon, G., Giddings, M.C., Ruan, Y., Wold, B., Carninci, P., Guigó, R., Gingeras, T.R.: Landscape of transcription in human cells. *Nature* **489**, 101–108 (2012). doi:[10.1038/nature11233](https://doi.org/10.1038/nature11233)
 22. Cocquerelle, C., Mascrez, B., Hétuin, D., Bailleul, B.: Mis-splicing yields circular RNA molecules. *FASEB J.* **7**(1), 155–160 (1993). doi:[10.1096/fasebj.7.1.7678559](https://doi.org/10.1096/fasebj.7.1.7678559)
 23. Qian, L., Vu, M.N., Carter, M., Wilkinson, M.F.: A spliced intron accumulates as a lariat in the nucleus of T cells. *Nucleic Acids Research* **20**(20), 5345–5350 (1992). doi:[10.1093/nar/20.20.5345](https://doi.org/10.1093/nar/20.20.5345). <https://academic.oup.com/nar/article-pdf/20/20/5345/7073334/20-20-5345.pdf>
 24. Thomas, L.F., Sætrom, P.: Circular RNAs are depleted of polymorphisms at microRNA binding sites. *Bioinformatics* **30**(16), 2243–2246 (2014). doi:[10.1093/bioinformatics/btu257](https://doi.org/10.1093/bioinformatics/btu257). <https://academic.oup.com/bioinformatics/article-pdf/30/16/2243/16918372/btu257.pdf>
 25. Hansen, T.B., Jensen, T.I., Clausen, B.H., Bramsen, J.B., Finsen, B., Damgaard, C.K., Kjems, J.: Natural RNA circles function as efficient microRNA sponges - Nature. *Nature* **495**, 384–388 (2013). doi:[10.1038/nature11993](https://doi.org/10.1038/nature11993)
 26. Denzler, R., Agarwal, V., Stefano, J., Bartel, D., Stoffel, M.: Assessing the cerna hypothesis with quantitative measurements of mirna and target abundance. *Molecular Cell* **54**(5), 766–776 (2014). doi:[10.1016/j.molcel.2014.03.045](https://doi.org/10.1016/j.molcel.2014.03.045)
 27. Aird, J., Baird, A.-M., Lim, M.C.J., McDermott, R., Finn, S.P., Gray, S.G.: Carcinogenesis in prostate cancer: The role of long non-coding RNAs. *Non-coding RNA Research* **3**(1), 29–38 (2018). doi:[10.1016/j.ncrna.2018.01.001](https://doi.org/10.1016/j.ncrna.2018.01.001)
 28. Bolton, E., Tuzova, A.V., Walsh, A.L., Lynch, T., Perry, A.S.: Noncoding RNAs in Prostate Cancer: The Long and the Short of It. *Clinical Cancer Research* **20**(1), 35–43 (2014). doi:[10.1158/1078-0432.CCR-13-1989](https://doi.org/10.1158/1078-0432.CCR-13-1989)
 29. Ghiam, A.F., Vesprini, D., Liu, S.K.: Long non-coding RNAs: new frontiers for advancing personalized cancer medicine in prostate cancer. *Translational Andrology and Urology* **6**(2), 32630–32330 (2017). doi:[10.21037/tau.2017.03.06](https://doi.org/10.21037/tau.2017.03.06)
 30. Ding, L., Wang, R., Shen, D., Cheng, S., Wang, H., Lu, Z., Zheng, Q., Wang, L., Xia, L., Li, G.: Role of noncoding RNA in drug resistance of prostate cancer. *Cell Death Dis.* **12**(590), 1–10 (2021). doi:[10.1038/s41419-021-03854-x](https://doi.org/10.1038/s41419-021-03854-x)
 31. Takayama, K.-i., Inoue, S.: The emerging role of noncoding RNA in prostate cancer progression and its implication on diagnosis and treatment. *Briefings in Functional Genomics* **15**(3), 257–265 (2015). doi:[10.1093/bfgp/elv057](https://doi.org/10.1093/bfgp/elv057). <https://academic.oup.com/bfg/article-pdf/15/3/257/6684852/elv057.pdf>
 32. Gonzalez, H., Hagerling, C., Werb, Z.: Roles of the immune system in

- cancer: from tumor initiation to metastatic progression. *Genes Dev.* **32**(19–20), 1267 (2018). doi:[10.1101/gad.314617.118](https://doi.org/10.1101/gad.314617.118)
33. Dieu-Nosjean, M.-C., Antoine, M., Danel, C., Heudes, D., Wislez, M., Poulot, V., Rabbe, N., Laurans, L., Tartour, E., de Chaisemartin, L., Lebecque, S., Fridman, W.-H., Cadranel, J.: Long-term survival for patients with non-small-cell lung cancer with intratumoral lymphoid structures. *J. Clin. Oncol.* **26**(27), 4410–4417 (2008). doi:[10.1200/JCO.2007.15.0284](https://doi.org/10.1200/JCO.2007.15.0284). 18802153
34. Mantovani, A., Marchesi, F., Malesci, A., Laghi, L., Allavena, P.: Tumor-Associated Macrophages as Treatment Targets in. *Nat. Rev. Clin. Oncol.* **14**(7), 399 (2017). doi:[10.1038/nrclinonc.2016.217](https://doi.org/10.1038/nrclinonc.2016.217)
35. Apusiga, K.: Immune cell infiltration-based prognosis in prostate cancer: a review of current knowledge. *Bull. Natl. Res. Cent.* **47**(1), 1–14 (2023). doi:[10.1186/s42269-023-01106-w](https://doi.org/10.1186/s42269-023-01106-w)
36. Edgar, R., Domrachev, M., Lash, A.E.: Gene Expression Omnibus: NCBI gene expression and hybridization array data repository. *Nucleic Acids Res.* **30**(1), 207–210 (2002). doi:[10.1093/nar/30.1.207](https://doi.org/10.1093/nar/30.1.207)
37. Jain, S., Lyons, C.A., Walker, S.M., McQuaid, S., Hynes, S.O., Mitchell, D.M., Pang, B., Logan, G.E., McCavigan, A.M., O'Rourke, D., McArt, D.G., McDade, S.S., Mills, I.G., Prise, K.M., Knight, L.A., Steele, C.J., Medlow, P.W., Berge, V., Katz, B., Loblaw, D.A., Harkin, D.P., James, J.A., O'Sullivan, J.M., Kennedy, R.D., Waugh, D.J.: Validation of a Metastatic Assay using biopsies to improve risk stratification in patients with prostate cancer treated with radical radiation therapy. *Ann. Oncol.* **29**(1), 215–222 (2018). doi:[10.1093/annonc/mdx637](https://doi.org/10.1093/annonc/mdx637). 29045551
38. Fraser, M., Sabelnykova, V.Y., Yamaguchi, T.N., Heisler, L.E., Livingstone, J., Huang, V., Shah, Y.-J., Yousif, F., Lin, X., Masella, A.P., Fox, N.S., Xie, M., Prokopcz, S.D., Berlin, A., Lalonde, E., Ahmed, M., Trudel, D., Luo, X., Beck, T.A., Meng, A., Zhang, J., D'Costa, A., Denroche, R.E., Kong, H., Espiritu, S.M.G., Chua, M.L.K., Wong, A., Chong, T., Sam, M., Johns, J., Timms, L., Buchner, N.B., Orain, M., Picard, V., Hovington, H., Murison, A., Kron, K., Harding, N.J., P'ng, C., Houlahan, K.E., Chu, K.C., Lo, B., Nguyen, F., Li, C.H., Sun, R.X., de Borja, R., Cooper, C.I., Hopkins, J.F., Govind, S.K., Fung, C., Waggett, D., Green, J., Haider, S., Chan-Seng-Yue, M.A., Jung, E., Wang, Z., Bergeron, A., Dal Pra, A., Lacombe, L., Collins, C.C., Sahinalp, C., Lupien, M., Fleshner, N.E., He, H.H., Fradet, Y., Tetu, B., van der Kwast, T., McPherson, J.D., Bristow, R.G., Boutros, P.C.: Genomic hallmarks of localized, non-indolent prostate cancer. *Nature* **541**, 359–364 (2017). doi:[10.1038/nature20788](https://doi.org/10.1038/nature20788)
39. Gerhauser, C., Favero, F., Risch, T., Simon, R., Feuerbach, L., Assenov, Y., Heckmann, D., Sidiropoulos, N., Waszak, S.M., Hübschmann, D., Urbanucci, A., Girma, E.G., Kuryshev, V., Klimczak, L.J., Saini, N., Stütz, A.M., Weichenhan, D., Böttcher, L.-M., Toth, R., Hendrikens, J.D., Koop, C., Lutsik, P., Matzke, S., Warnatz, H.-J., Amstislavskiy, V., Feuerstein, C., Raeder, B., Bogatyrova, O., Schmitz, E.-M., Hube-Magg, C., Kluth, M., Huland, H., Graefen, M., Lawerenz, C., Henry, G.H., Yamaguchi, T.N., Malewska, A., Meiners, J., Schilling, D., Reisinger, E., Eils, R., Schlesner, M., Strand, D.W., Bristow, R.G., Boutros, P.C., von Kalle, C., Gordenin, D., Sültmann, H., Brors, B., Sauter, G., Plass, C., Yaspo, M.-L., Korbel, J.O., Schlomm, T., Weischenfeldt, J.: Molecular Evolution of Early-Onset Prostate Cancer Identifies Molecular Risk Markers and Clinical Trajectories. *Cancer Cell* **34**(6), 996–1018 (2018). doi:[10.1016/j.ccr.2018.10.016](https://doi.org/10.1016/j.ccr.2018.10.016). 30537516
40. Long, Q., Xu, J., Osunkoya, A.O., Sannigrahi, S., Johnson, B.A., Zhou, W., Gillespie, T., Park, J.Y., Nam, R.K., Sugar, L., Stanimirovic, A., Seth, A.K., Petros, J.A., Moreno, C.S.: Global Transcriptome Analysis of Formalin-Fixed Prostate Cancer Specimens Identifies Biomarkers of Disease Recurrence. *Cancer Res.* **74**(12), 3228–3237 (2014). doi:[10.1158/0008-5472.CAN-13-2699](https://doi.org/10.1158/0008-5472.CAN-13-2699)
41. Taylor, B.S., Schultz, N., Hieronymus, H., Gopalan, A., Xiao, Y., Carver, B.S., Arora, V.K., Kaushik, P., Cerami, E., Reva, B., Antipin, Y., Mitsiadis, N., Landers, T., Dolgalev, I., Major, J.E., Wilson, M., Soccia, N.D., Lash, A.E., Heguy, A., Eastham, J.A., Scher, H.I., Reuter, V.E., Scardino, P.T., Sander, C., Sawyers, C.L., Gerald, W.L.: Integrative Genomic Profiling of Human Prostate Cancer. *Cancer Cell* **18**(1), 11–22 (2010). doi:[10.1016/j.ccr.2010.05.026](https://doi.org/10.1016/j.ccr.2010.05.026)
42. Ross-Adams, H., Lamb, A.D., Dunning, M.J., Halim, S., Lindberg, J., Massie, C.M., Egevad, L.A., Russell, R., Ramos-Montoya, A., Vowler, S.L., Sharma, N.L., Kay, J., Whitaker, H., Clark, J., Hurst, R., Gnanapragasam, V.J., Shah, N.C., Warren, A.Y., Cooper, C.S., Lynch, A.G., Stark, R., Mills, I.G., Grönberg, H., Neal, D.E., CamCaP Study Group: Integration of copy number and transcriptomics provides risk stratification in prostate cancer: A discovery and validation cohort study. *EBioMedicine* **2**(9), 1133–1144 (2015). doi:[10.1016/j.ebiom.2015.07.017](https://doi.org/10.1016/j.ebiom.2015.07.017). 26501111
43. Davis, S., Meltzer, P.S.: GEOquery: a bridge between the Gene Expression Omnibus (GEO) and BioConductor. *Bioinformatics* **23**(14), 1846–1847 (2007). doi:[10.1093/bioinformatics/btm254](https://doi.org/10.1093/bioinformatics/btm254)
44. Parkinson, H., Kapushesky, M., Shojatalab, M., Abeygunawardena, N., Coulson, R., Farne, A., Holloway, E., Kolesnykov, N., Lilja, P., Lukk, M., Mani, R., Rayner, T., Sharma, A., William, E., Sarkans, U., Brazma, A.: ArrayExpress—a public database of microarray experiments and gene expression profiles. *Nucleic Acids Res.* **35**(Database), 747 (2007). doi:[10.1093/nar/gkl995](https://doi.org/10.1093/nar/gkl995)
45. Carvalho, B.S., Irizarry, R.A.: A framework for oligonucleotide microarray preprocessing. *Bioinformatics* **26**(19), 2363–2367 (2010). doi:[10.1093/bioinformatics/btp431](https://doi.org/10.1093/bioinformatics/btp431)
46. Robinson, M.D., McCarthy, D.J., Smyth, G.K.: edgeR: a Bioconductor package for differential expression analysis of digital gene expression data. *Bioinformatics* **26**(1), 139–140 (2010). doi:[10.1093/bioinformatics/btp616](https://doi.org/10.1093/bioinformatics/btp616)
47. Law, C.W., Chen, Y., Shi, W., Smyth, G.K.: voom: precision weights unlock linear model analysis tools for RNA-seq read counts. *Genome Biol.* **15**(2), 1–17 (2014). doi:[10.1186/gb-2014-15-2-r29](https://doi.org/10.1186/gb-2014-15-2-r29)
48. Langmead, B., Trapnell, C., Pop, M., Salzberg, S.L.: Ultrafast and memory-efficient alignment of short DNA sequences to the human genome. *Genome Biol.* **10**(3), 1–10 (2009). doi:[10.1186/gb-2009-10-3-r25](https://doi.org/10.1186/gb-2009-10-3-r25)
49. Shen, W., Le, S., Li, Y., Hu, F.: SeqKit: A Cross-Platform and Ultrafast Toolkit for FASTA/Q File Manipulation. *PLoS One* **11**(10), 0163962 (2016). doi:[10.1371/journal.pone.0163962](https://doi.org/10.1371/journal.pone.0163962)
50. Krueger, F., James, F., Ewels, P., Afyounian, E., Weinstein, M., Schuster-Boeckler, B., Hulselmans, G., sclamons: FelixKrueger/TrimGalore: v0.6.10. Zenodo (2023). doi:[10.5281/zenodo.7598955](https://doi.org/10.5281/zenodo.7598955)
51. Pantano, L., Friedländer, M.R., Escaramís, G., Lizano, E., Pallarès-Albanell, J., Ferrer, I., Estivill, X., Martí, E.: Specific small-RNA signatures in the amygdala at premotor and motor stages of Parkinson's disease revealed by deep sequencing analysis. *Bioinformatics* **32**(5), 673–681 (2016). doi:[10.1093/bioinformatics/btv632](https://doi.org/10.1093/bioinformatics/btv632)
52. Desvignes, T., Loher, P., Eilbeck, K., Ma, J., Urgese, G., Fromm, B., Sydes, J., Aparicio-Puerta, E., Barrera, V., Espín, R., Thibord, F., Bofill-De Ros, X., Londin, E., Telonis, A.G., Ficarra, E., Friedländer, M.R., Postlethwait, J.H., Rigoutsos, I., Hackenberg, M., Vlachos, I.S., Halushka, M.K., Pantano, L.: Unification of miRNA and isomiR research: the mirGFF3 format and the mirtop API. *Bioinformatics* **36**(3), 698–703 (2020). doi:[10.1093/bioinformatics/btz675](https://doi.org/10.1093/bioinformatics/btz675)
53. Patel, H., Ewels, P., Peltzer, A., Botvinnik, O., Sturm, G., Moreno, D., Vemuri, P., Garcia, M.U., silviamorins, Pantano, L., Binzer-Panchal, M., Bot, N.-C., Syme, R., Zepper, M., Kelly, G., Hanssen, F., Yates, J.A.F., Cheshire, C., rfenouil, Espinosa-Carrasco, J., marcheppner, Miller, E., Talbot, A., Zhou, P., Guinchard, S., Hörttenhuber, M., Gabernet, G., Mertes, C., Straub, D., Di Tommaso, P.: nf-core/rnaseq: nf-core/rnaseq v3.12.0 - Osmium Octopus. Zenodo (2023). doi:[10.5281/zenodo.7998767](https://doi.org/10.5281/zenodo.7998767)
54. Ritchie, M.E., Phipson, B., Wu, D., Hu, Y., Law, C.W., Shi, W., Smyth, G.K.: limma powers differential expression analyses for RNA-sequencing and microarray studies. *Nucleic Acids Res.* **43**(7), 47 (2015). doi:[10.1093/nar/gkv007](https://doi.org/10.1093/nar/gkv007)
55. Glažar, P., Papavasileiou, P., Rajewsky, N.: circBase: a database for circular RNAs. *RNA* **20**(11), 1666 (2014). doi:[10.1261/rna.043687.113](https://doi.org/10.1261/rna.043687.113)
56. Xia, S., Feng, J., Chen, K., Ma, Y., Gong, J., Cai, F., Jin, Y., Gao, Y., Xia, L., Chang, H., Wei, L., Han, L., He, C.: CSCD: a database for cancer-specific circular RNAs. *Nucleic Acids Res.* **46**(Database), 925 (2018). doi:[10.1093/nar/gkx863](https://doi.org/10.1093/nar/gkx863)
57. Kozomara, A., Birgaoanu, M., Griffiths-Jones, S.: miRBase: from microRNA sequences to function. *Nucleic Acids Res.* **47**(D1), 155–162 (2019). doi:[10.1093/nar/gky1141](https://doi.org/10.1093/nar/gky1141)

58. Hsu, S.-D., Lin, F.-M., Wu, W.-Y., Liang, C., Huang, W.-C., Chan, W.-L., Tsai, W.-T., Chen, G.-Z., Lee, C.-J., Chiu, C.-M., Chien, C.-H., Wu, M.-C., Huang, C.-Y., Tsou, A.-P., Huang, H.-D.: miRTarBase: a database curates experimentally validated microRNA-target interactions. *Nucleic Acids Res.* **39**(Database), (2011). doi:[10.1093/nar/gkq1107.21071411](https://doi.org/10.1093/nar/gkq1107.21071411)
59. Chang, L., Zhou, G., Soufan, O., Xia, J.: miRNet 2.0: network-based visual analytics for miRNA functional analysis and systems biology. *Nucleic Acids Res.* **48**(W1), 244–251 (2020). doi:[10.1093/nar/gkaa467](https://doi.org/10.1093/nar/gkaa467)
60. Agarwal, V., Bell, G.W., Nam, J.-W., Bartel, D.P.: Predicting effective microRNA target sites in mammalian mRNAs. *eLife* (2015). doi:[10.7554/eLife.05005](https://doi.org/10.7554/eLife.05005)
61. Shannon, P., Markiel, A., Ozier, O., Baliga, N.S., Wang, J.T., Ramage, D., Amin, N., Schwikowski, B., Ideker, T.: Cytoscape: A Software Environment for Integrated Models of Biomolecular Interaction Networks. *Genome Res.* **13**(11), 2498 (2003). doi:[10.1101/gr.1239303](https://doi.org/10.1101/gr.1239303)
62. Ulgen, E., Ozisik, O., Sezerman, O.U.: pathfindR: An R Package for Comprehensive Identification of Enriched Pathways in Omics Data Through Active Subnetworks. *Front. Genet.* **10**, 425394 (2019). doi:[10.3389/fgene.2019.00858](https://doi.org/10.3389/fgene.2019.00858)
63. Blighe, K.: RegParallel. [Online; accessed 12. Sep. 2023] (2023). <https://biocconductor.org/packages/release/data/experiment/html/RegParallel.html>
64. Schoenfeld, D.: Partial residuals for the proportional hazards regression model. *Biometrika* **69**(1), 239–241 (1982). doi:[10.1093/biomet/69.1.239](https://doi.org/10.1093/biomet/69.1.239)
65. Venables, W.N., Ripley, B.D.: Modern Applied Statistics with S, 4th edn. Springer, New York (2002). ISBN 0-387-95457-0. <https://www.stats.ox.ac.uk/pub/MASS4/>
66. Kassambara, A.: Drawing Survival Curves using 'ggplot2' [R package survminer version 0.4.9]. Comprehensive R Archive Network (CRAN). [Online; accessed 25. Aug. 2023] (2021). <https://cran.r-project.org/web/packages/survminer/index.html>
67. Blanché, P.: timeROC: Time-Dependent ROC Curve and AUC for Censored Survival Data. Comprehensive R Archive Network (CRAN). [Online; accessed 25. Aug. 2023] (2023). <https://cran.r-project.org/web/packages/timeROC/index.html>
68. Hothorn, T.: maxstat: Maximally Selected Rank Statistics. Comprehensive R Archive Network (CRAN). [Online; accessed 12. Sep. 2023] (2017). <https://cran.r-project.org/web/packages/maxstat>
69. Harrell, F.E. Jr.: Harrell Miscellaneous [R package Hmisc version 5.1-1]. Comprehensive R Archive Network (CRAN) (2023)
70. Harrell, F.E. Jr.: rms: Regression Modeling Strategies. Comprehensive R Archive Network (CRAN). [Online; accessed 19. Sep. 2023] (2023). <https://cran.r-project.org/web/packages/rms>
71. Marshall, R.: Enhanced Regression Nomogram Plot [R package regplot version 1.1]. Comprehensive R Archive Network (CRAN) (2020)
72. Royston, P., Altman, D.G.: External validation of a Cox prognostic model: principles and methods. *BMC Med. Res. Method.* **13**(1), 1–15 (2013). doi:[10.1186/1471-2288-13-33](https://doi.org/10.1186/1471-2288-13-33)
73. Yoshihara, K., Shahmoradgoli, M., Martínez, E., Vegesna, R., Kim, H., Torres-García, W., Treviño, V., Shen, H., Laird, P.W., Levine, D.A., Carter, S.L., Getz, G., Stemke-Hale, K., Mills, G.B., Verhaak, R.G.W.: Inferring tumour purity and stromal and immune cell admixture from expression data. *Nat. Commun.* **4**(2612), 1–11 (2013). doi:[10.1038/ncomms3612](https://doi.org/10.1038/ncomms3612)
74. Hänelmann, S., Castelo, R., Guinney, J.: GSVA: gene set variation analysis for microarray and RNA-Seq data. *BMC Bioinf.* **14**(1), 1–15 (2013). doi:[10.1186/1471-2105-14-7](https://doi.org/10.1186/1471-2105-14-7)
75. Ahmad, F., Cherukuri, M.K., Choyke, P.L.: Metabolic reprogramming in prostate cancer. *Br. J. Cancer* **125**, 1185–1196 (2021). doi:[10.1038/s41416-021-01435-5](https://doi.org/10.1038/s41416-021-01435-5)
76. Luo, L., Zhang, L.-L., Tao, W., Xia, T.-L., Li, L.-Y.: Prediction of potential prognostic biomarkers in metastatic prostate cancer based on a circular RNA-mediated competing endogenous RNA regulatory network. *PLoS One* **16**(12), 0260983 (2021). doi:[10.1371/journal.pone.0260983](https://doi.org/10.1371/journal.pone.0260983)
77. Zhang, X.-Y., Mao, L.: Circular RNA Circ_0000442 acts as a sponge of MiR-148b-3p to suppress breast cancer via PTEN/PI3K/Akt signaling pathway. *Gene* **766**, 145113 (2021). doi:[10.1016/j.gene.2020.145113](https://doi.org/10.1016/j.gene.2020.145113)
78. Zhu, K.-P., Zhang, C.-L., Ma, X.-L., Hu, J.-P., Cai, T., Zhang, L.: Analyzing the Interactions of mRNAs and ncRNAs to Predict Competing Endogenous RNA Networks in Osteosarcoma Chemo-Resistance. *Mol. Ther.* **27**(3), 518–530 (2019). doi:[10.1016/j.ymthe.2019.01.001](https://doi.org/10.1016/j.ymthe.2019.01.001)
79. Hoey, C., Ray, J., Jeon, J., Huang, X., Taeb, S., Ylanko, J., Andrews, D.W., Boutros, P.C., Liu, S.K.: miRNA-106a and prostate cancer radioresistance: a novel role for LITAF in ATM regulation. *Mol. Oncol.* **12**(8), 1324–1341 (2018). doi:[10.1002/1878-0261.12328](https://doi.org/10.1002/1878-0261.12328)
80. Guo, K., Zheng, S., Xu, Y., Xu, A., Chen, B., Wen, Y.: Loss of miR-26a-5p promotes proliferation, migration, and invasion in prostate cancer through negatively regulating SERBP1. *Tumor Biol.* **37**(9), 12843–12854 (2016). doi:[10.1007/s13277-016-5158-z](https://doi.org/10.1007/s13277-016-5158-z)
81. Chen, Y.-T., Huang, C.-R., Chang, C.-L., Chiang, J.Y., Luo, C.-W., Chen, H.-H., Yip, H.-K.: Jagged2 progressively increased expression from Stage I to III of Bladder Cancer and Melatonin-mediated downregulation of Notch/Jagged2 suppresses the Bladder Tumorigenesis via inhibiting PI3K/AKT/mTOR/MMPs signaling. *Int. J. Biol. Sci.* **16**(14), 2648–2662 (2020). doi:[10.7150/ijbs.48358.32792862](https://doi.org/10.7150/ijbs.48358.32792862)
82. Yang, Y., Ahn, Y.-H., Gibbons, D.L., Zang, Y., Lin, W., Thilaganathan, N., Alvarez, C.A., Moreira, D.C., Creighton, C.J., Gregory, P.A., Goodall, G.J., Kurie, J.M.: The Notch ligand Jagged2 promotes lung adenocarcinoma metastasis through a miR-200-dependent pathway in mice. *J. Clin. Invest.* **121**(4), 1373–1385 (2011). doi:[10.1172/JCI42579.21403400](https://doi.org/10.1172/JCI42579.21403400)
83. Vaish, V., Kim, J., Shim, M.: Jagged-2 (JAG2) enhances tumorigenicity and chemoresistance of colorectal cancer cells. *Oncotarget* **8**(32), 53262 (2017). doi:[10.18632/oncotarget.18391](https://doi.org/10.18632/oncotarget.18391)
84. Ross, A.E., Marchionni, L., Vuica-Ross, M., Cheadle, C., Fan, J., Berman, D.M., Schaeffer, E.M.: Gene expression pathways of high grade localized prostate cancer. *Prostate* **71**(14), 1568–1577 (2011). doi:[10.1002/pros.21373](https://doi.org/10.1002/pros.21373)
85. Ma, Z., Chao, F., Wang, S., Song, Z., Zhuo, Z., Zhang, J., Xu, G., Chen, G.: CTHRC1 affects malignant tumor cell behavior and is regulated by miR-30e-5p in human prostate cancer. *Biochem. Biophys. Res. Commun.* **525**(2), 418–424 (2020). doi:[10.1016/j.bbrc.2020.02.098](https://doi.org/10.1016/j.bbrc.2020.02.098)
86. Ohara, S., Oue, N., Matsubara, A., Mita, K., Hasegawa, Y., Hayashi, T., Usui, T., Amatya, V.J., Takeshima, Y., Kuniyasu, H., Yasui, W.: Reg IV is an independent prognostic factor for relapse in patients with clinically localized prostate cancer. *Cancer Sci.* **99**(8), 1570–1577 (2008). doi:[10.1111/j.1349-7006.2008.00846.x](https://doi.org/10.1111/j.1349-7006.2008.00846.x)
87. Gu, Z., Rubin, M.A., Yang, Y., Deprimo, S.E., Zhao, H., Horvath, S., Brooks, J.D., Loda, M., Reiter, R.E.: Reg IV: A Promising Marker of Hormone Refractory Metastatic Prostate Cancer. *Clin. Cancer Res.* **11**(6), 2237–2243 (2005). doi:[10.1158/1078-0432.CCR-04-0356](https://doi.org/10.1158/1078-0432.CCR-04-0356)
88. Lee, J.O., Lee, S.K., Kim, J.H., Kim, N., You, G.Y., Moon, J.W., Kim, S.J., Park, S.H., Kim, H.S.: Metformin Regulates Glucose Transporter 4 (GLUT4) Translocation through AMP-activated Protein Kinase (AMPK)-mediated Cbl/CAP Signaling in 3T3-L1 Preadipocyte Cells. *J. Biol. Chem.* **287**(53), 44121 (2012). doi:[10.1074/jbc.M112.361386](https://doi.org/10.1074/jbc.M112.361386)
89. Spratt, D.E., Zhang, C., Zumsteg, Z.S., Pei, X., Zhang, Z., Zelefsky, M.J.: Metformin and Prostate Cancer: Reduced Development of Castration-resistant Disease and Prostate Cancer Mortality. *Eur. Urol.* **63**(4), 709–716 (2013). doi:[10.1016/j.euro.2012.12.004](https://doi.org/10.1016/j.euro.2012.12.004)
90. Colquhoun, A.J., Venier, N.A., Vandersluis, A.D., Besla, R., Sugar, L.M., Kiss, A., Fleshner, N.E., Pollak, M., Klotz, L.H., Venkateswaran, V.: Metformin enhances the antiproliferative and apoptotic effect of bicalutamide in prostate cancer. *Prostate Cancer Prostatic Dis.* **15**(4), 346–352 (2012). doi:[10.1038/pcan.2012.16.22614062](https://doi.org/10.1038/pcan.2012.16.22614062)
91. Liu, Q., Tong, D., Liu, G., Xu, J., Do, K., Geary, K., Zhang, D., Zhang, J., Zhang, Y., Li, Y., Bi, G., Lan, W., Jiang, J.: Metformin reverses prostate cancer resistance to enzalutamide by targeting TGF- β 1/STAT3 axis-regulated EMT. *Cell Death Dis.* **8**(8) (2017). doi:[10.1038/cddis.2017.417](https://doi.org/10.1038/cddis.2017.417)